MOUNTAIN-PLAINS CONSORTIUM

MPC 24-544 | R. Ghabchi and M. Castro

DEVELOPMENT AND CHARACTERIZATION OF A PLANT-BASED BIO-ADDITIVE FOR ASPHALT BINDER

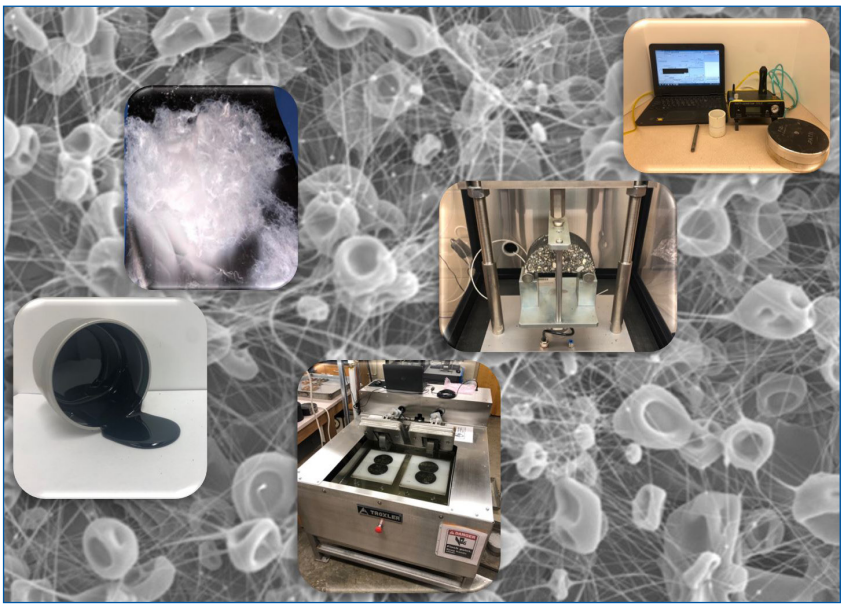

MOUNTAIN-PLAINS CONSORTIUM REGION 8

A University Transportation Center sponsored by the U.S. Department of Transportation serving the Mountain-Plains Region. Consortium members:

Colorado State University
North Dakota State University
South Dakota State University
University of Colorado Denver
University of Denver
University of Utah
Utah State University
University of Wyoming

Technical Report Documentation Page

1. Report No.	2. Government Accession No.	3. Recipient's Catalog No.
MPC-575		

4. Title and Subtitle	5. Report Date
Development and Characterization of a Plant-based Bio-Additive for Asphalt Binder	August 2024
	6. Performing Organization Code

7. Author(s)	8. Performing Organization Report No.
Rouzbeh Ghabchi, Ph.D., PE Marco Paulo Pereira Castro	MPC 24-544

9. Performing Organization Name and Address	10. Work Unit No. (TRAIS)
Department of Civil and Environmental Engineering South Dakota State University Brookings, SD 57007	11. Contract or Grant No.

12. Sponsoring Agency Name and Address	13. Type of Report and Period Covered
Mountain-Plains Consortium North Dakota State University PO Box 6050, Fargo, ND 58108	Final Report
	14. Sponsoring Agency Code

15. Supplementary Notes

Supported by a grant from the US DOT, University Transportation Centers Program

16. Abstract

In recent years, major initiatives have been taken to replace non-renewable materials with environmentally friendly and sustainable ones. The present study was undertaken to apply a scalable process for laboratory production of cellulose nanofibers (CNF) and to evaluate the feasibility of using the produced CNF as a sustainable plant-based asphalt additive to improve the mechanical properties and durability of asphalt pavements. CNF was produced in the laboratory by applying an electrospinning technique to achieve this goal. Structure, morphology, and the size distribution of the produced CNF were evaluated using scan electron microscopy. Also, tensile strength tests in two perpendicular directions were conducted on lab-produced CNF. The effect of incorporating different amounts of CNF in three types of asphalt binders, PG 58-28, PG 64-34, and PG 70-28, on fracture energy and dynamic viscosity of binder blends were evaluated by conducting Izod impact and rotational viscometer tests, respectively. Additionally, the effect of CNF dosage in the binder on its adhesion and moisture-induced debonding potential of three different mineralogy aggregates was evaluated by conducting a binder bond strength test. Furthermore, the effect of incorporating CNF in asphalt mixes on their cracking, rutting, and moisture-induced damage potential was evaluated by conducting semi-circular bend, Hamburg wheel tracking, and tensile strength ratio tests. The tests conducted on asphalt binders and mixes revealed that incorporation of CNF resulted in an overall improvement in binder-aggregates adhesion, an asphalt binder with a higher fracture energy and dynamic viscosity, and an asphalt mix with a higher resistance to rutting, cracking, and moisture-induced damage.

17. Key Word	18. Distribution Statement
additives, asphalt pavements, binder content, bituminous binders, evaluation and assessment, feasibility analysis, laboratory tests, vegetable materials, waste products	Public distribution

19. Security Classif. (of this report)	20. Security Classif. (of this page)	21. No. of Pages	22. Price
Unclassified	Unclassified	60	n/a

DEVELOPMENT AND CHARACTERIZATION OF A PLANT-BASED BIO-ADDITIVE FOR ASPHALT BINDER

Rouzbeh Ghabchi, Ph.D., P.E.
Associate Professor
Department of Civil and Environmental Engineering
South Dakota State University
Brookings, SD 57007

Marco Paulo Pereira Castro
Graduate Research Assistant
Department of Civil and Environmental Engineering
South Dakota State University
Brookings, SD 57007

August 2024

Acknowledgment

The study presented herein was conducted with support from the Mountain-Plains Consortium (MPC), a University Transportation Center funded by the United States Department of Transportation through project MPC-575. Contributions of the Ingevity Co., Bowes Construction Co., Jebro Co., Flint Hills Co., and GCC Ready Mix Co. are highly appreciated.

Disclaimer

ABSTRACT

In recent years, major initiatives have been taken to replace non-renewable materials with environmentally friendly and sustainable ones. The present study was undertaken to apply a scalable process for laboratory production of cellulose nanofibers (CNF) and to evaluate the feasibility of using the produced CNF as a sustainable plant-based asphalt additive to improve the mechanical properties and durability of asphalt pavements. CNF was produced in the laboratory by applying an electrospinning technique to achieve this goal. Structure, morphology, and the size distribution of the produced CNF were evaluated using scan electron microscopy. Also, tensile strength tests in two perpendicular directions were conducted on lab-produced CNF. The effect of incorporating different amounts of CNF in three types of asphalt binders, PG 58-28, PG 64-34, and PG 70-28, on fracture energy and dynamic viscosity of binder blends were evaluated by conducting Izod impact and rotational viscometer tests, respectively. Additionally, the effect of CNF dosage in the binder on its adhesion and moisture-induced debonding potential of three different mineralogy aggregates was evaluated by conducting a binder bond strength test. Furthermore, the effect of incorporating CNF in asphalt mixes on their cracking, rutting, and moisture-induced damage potential was evaluated by conducting semi-circular bend, Hamburg wheel tracking, and tensile strength ratio tests. The tests conducted on asphalt binders and mixes revealed that incorporation of CNF resulted in an overall improvement in binder-aggregates adhesion, an asphalt binder with a higher fracture energy and dynamic viscosity, and an asphalt mix with a higher resistance to rutting, cracking, and moisture-induced damage.
.

TABLE OF CONTENTS

LIST OF TABLES

LIST OF FIGURES

EXECUTIVE SUMMARY

Asphalt binder used for pavement construction is obtained mainly by distilling crude oil in refineries. The scarcity of natural resources, environmental concerns, and emerging needs for sustainable materials have spurred the development and use of materials and processes that are renewable and environmentally friendly. In response to this need, initiatives have been taken to develop a new generation of bio-based construction materials because of continuous innovation in using agricultural products, byproducts, and biomass as a material feedstock. The development of biomaterials to replace their petroleum-based counterparts is a major element of these initiatives. Therefore, developing and evaluating innovative plant-based asphalt additives, such as cellulose and lignin, will help increase the use of biomaterials to maximize the sustainability of the ground transportation system. This study evaluated cellulose nanofibers (CNF) as an asphalt binder additive derived from agricultural products and byproducts prevailing in the North Central Region (e.g., corn and soybean) as the primary feedstock. This objective was achieved through a laboratory testing program to evaluate the performance of asphalt mixes containing plant-based CNF. More specifically, the present study was undertaken to apply a scalable process for laboratory production of CNF and to evaluate the feasibility of using the produced CNF as a sustainable plant-based asphalt additive to improve the mechanical properties and durability of asphalt pavements. CNF was produced in the laboratory by applying an electrospinning technique to achieve this goal. Structure, morphology, and size distribution of the produced CNF were evaluated using scan electron microscopy. Also, tensile strength tests in two perpendicular directions were conducted on lab-produced CNF. The effect of incorporating different CNF amounts in three types of asphalt binders, PG 58-28, PG 64-34, and PG 70-28, on fracture energy and dynamic viscosity of binder blends was evaluated by conducting Izod impact and rotational viscometer tests, respectively. Additionally, the effect of CNF dosage in the binder on its adhesion and moisture-induced debonding potential of three different mineralogy aggregates was evaluated by conducting a binder bond strength test. Furthermore, the effect of incorporating CNF in asphalt mixes on their cracking, rutting, and moisture-induced damage potential was evaluated by conducting semi-circular bend, Hamburg wheel tracking, and tensile strength ratio tests. The tests conducted on asphalt binders and mixes revealed that incorporation of CNF resulted in an overall improvement in binder-aggregates adhesion, an asphalt binder with a higher fracture energy and dynamic viscosity, and an asphalt mix with a higher resistance to rutting, cracking, and moisture-induced damage. The study's findings allowed the research team to collect the necessary data to assess the feasibility of using these materials in the construction of asphalt pavements in South Dakota and elsewhere. This study is further expected to promote the use of sustainable biomaterials and agricultural byproducts as the primary feedstock for producing bio-based asphalt binder additives. After implementation, this is expected to result in less need for petroleum-based products, which will lead to numerous environmental benefits. In addition, due to the availability of biomaterials and their low cost, significant cost savings are projected from the outcomes of this project.

1. INTRODUCTION

1.1 Problem Statement

Approximately 2.4 million miles of paved roads are constructed in the United States with hot mix asphalt (HMA). Asphalt binder is a viscoelastic and thermoplastic material obtained from the distillation of naturally occurring crude oil and is responsible for the binding and viscoelastic behavior of the HMA. Many aspects of pavement performance, such as resistance to permanent deformation (rutting), thermal cracking, fatigue life, and stripping, are significantly influenced by the mechanical and chemical properties of the asphalt binder.

Asphalt pavements face severe distress due to traffic and environmental conditions during their service life. Repeated vehicular loading occurs on pavement, causing accumulation and growth of micro and macro cracks due to fatigue. Asphalt pavements can withstand repeated bending without fracturing (Moghadas Nejad et al., 2010). However, the asphalt pavement's fatigue failure is observed as cracks with increased traffic loading. The quest to improve pavement performance has led to the development and use of a wide range of asphalt binders and mix modifiers. Polymer-modified asphalt binder is an effective means to enhance pavement performance (Yildirim, 2007). However, the development and use of polymer-modified asphalt binders are challenging due to their high cost compared with unmodified asphalt binders. Also, the poor asphalt polymer compatibility (which influences the system's stability) and the higher viscosities during asphalt processing and application make it challenging to use polymer-modified asphalt binder.

With new asphalt technologies introduced over the last 20 years, new materials and methods have been developed as alternative sources to replace and reduce petroleum-based asphalt binders and additives used in HMA. New materials and techniques are necessary to overcome the scarcity of natural resources, oil price increases, emerging environmental concerns, and the necessity for sustainable materials that are renewable and environmentally friendly. Among those alternatives, mixes containing reclaimed asphalt pavement (RAP) and renewable and bio-based materials are being studied to modify asphalt binders. These available alternatives are economically efficient and environmentally sustainable. The use of RAP in 2022 conserved approximately 26.9 million barrels of asphalt binder. The use of RAP in new pavement construction also conserved more than 84.3 million metric tons of aggregate and reduced the amount of construction waste sent to landfills by 52.1 million cubic meters (Williams et al., 2024)

Cellulose acetate (CA), a bio-based material, is an important ester of cellulose. It is obtained by the reaction of cellulose with acetic anhydride and acetic acid in the presence of sulfuric acid. It can be used for various applications, including fiber production such as cellulose nano-fibers (CNFs). The CA is soluble in acetone and acetic acid (Fischer et al., 2008). Due to its mechanical strength and biocompatibility, nanocrystalline cellulose has been used as reinforcement polymer matrices for some applications. The goal is to improve the rheological properties of asphalt binders by incorporating CNFs, improving the performance of asphalt mixes against pavement distresses. Nano-reinforced materials hold the potential to help the pavement industry improve the performance and sustainability of asphalt pavements. Due to the absence of widely accepted standards for the production and incorporation of CNF in asphalt binder and mixes and the lack of laboratory test results, CNF as an asphalt additive has not been explored.

CNF production by electrospinning CA has attracted significant attention due to its good thermal stability, chemical resistance, and biodegradability. The electrospinning technique was applied to produce CNF to modify the asphalt binder and mix. Electrospinning is a technique that utilizes electrical forces to produce polymer fibers with diameters ranging from 2 nm to several micrometers using polymer solutions. It is a unique approach that uses electrostatic forces and high voltage to produce fibers from polymer solutions. It is a robust and straightforward technique to produce nanofibers from various polymers (Li and Xia,

2004). Fibers produced using the electrospinning technique have several advantages, such as an extremely high surface-to-volume ratio, tunable porosity, malleability to conform to a wide variety of sizes and shapes, and the ability to control the nanofiber composition to achieve the desired characteristics (Bhardwaj and Kundu, 2010). The basic setup of electrospinning consists of a high-voltage power supply, a spinneret (metallic needle), and a collector (grounded conductor) (Li and Xia, 2004).

In this study, to promote the use of sustainable biomaterials and agricultural byproducts as the primary feedstock for the production of bio-asphalt binder, electrospun cellulose nanofiber was used as a substitute for the conventional polymers to improve the performance of asphalt mix. Laboratory testing was conducted to determine the fibers' structure and effects on the asphalt binder and mix. Scanning electron microscopy (SEM) was used to characterize the fibers' size and morphological features. In order to characterize the resistance of asphalt mixes to cracking, the semi-circular bend (SCB) test was conducted on the asphalt mixes containing CNF using an asphalt standard tester according to the ASTM D8044 test method. Hamburg wheel tracking (HWT) and tensile strength ratio (TSR) tests were also conducted on the samples to evaluate their resistance to rutting and moisture damage according to AASHTO T324 and AASHTO T283 standard methods. An Izod impact strength test was also conducted as an innovative method (ASTM D256) to determine the fracture energy of the asphalt binder containing cellulose nanofiber at low temperatures. A binder bond strength test was also conducted to evaluate the adhesion between the asphalt binder containing CNF and different aggregates following the AASHTO T 361 standard method. Finally, the optimum plant mixing and compaction temperatures for asphalt binders were determined by conducting a rotational viscosity test using the AASHTO T316 test method.

1.2 Research Objectives

The specific objectives of this study were as follows.

1. Production of CNF using static and rotating electrospinning fiber production techniques;
2. Characterization of the produced CNF, including identifying the optimum solvent, roughness, average diameter of the fiber, and tensile strength (consequently, the solution that will be used for the production of CNF to be incorporated in the mixes will be selected);
3. Evaluation of neat asphalt binder and CNF-modified asphalt binder;
4. Evaluation of asphalt mixes without any CNF and those containing different amounts of CNF.

1.3 Significance of Study

The present study was pursued to generate valuable laboratory test data of asphalt mixes containing CNF as an additive in asphalt binder. The test results are expected to help develop a modified plant-based bio-asphalt binder to replace the petroleum-based polymers used in the binder to maximize the sustainability of the ground transportation system.

1.4 Study Tasks

Specific tasks to be carried out in the study are as follows.

1. Prepare five different solutions, mixing cellulose acetate powder with a solvent for future production of CNF;
2. Produce CNF from the previously prepared solutions using the static and rotating electrospinning techniques;

3. Evaluate the roughness, entanglement, and average diameter of the produced CNF using the SEM technique;
4. Evaluate the average tensile strength of the different produced CNFs to select the optimum solution and electrospinning technique for the study;
5. Collect three types of asphalt binders, PG 58-28, PG 64-34, and PG 70-28, and produce modified binders by mixing the produced CNF with the collected asphalt binders;
6. Conduct Izod impact strength test following ASTM D256 (test method A) using a pendulum impact device on the neat asphalt binder and the CNF-modified asphalt binder;
7. Conduct RV test per AASHTO T316 test method using a Brookfield rotational viscometer on the unmodified binder and CNF-modified asphalt binders;
8. Conduct binder bond strength tests following AASHTO T 361 using a pneumatic adhesion tensile testing instrument (PATTI) on unconditioned and moisture-conditioned asphalt binder-aggregate samples;
9. Collect an HMA mix containing PG 58-28 asphalt binder, mainly quartzite and granite aggregates, and 20% RAP with a nominal maximum aggregate size (NMAS) of 12.5 mm;
10. Produce a CNF-modified asphalt mix with the collected asphalt for future laboratory testing;
11. Conduct TSR tests following AASHTO T 283 on unconditioned and moisture-conditioned asphalt mix specimens;
12. Conduct SCB tests following ASTM D8044 on dry and moisture-conditioned
13. Conduct HWT tests following AASHTO T324 on mixes containing CNF and those without CNF;
14. Evaluate the effect of the asphalt binder type, aggregate type, and percentage of fibers on adhesion of the asphalt binder with aggregates in moisture-conditioned and unconditioned states;
15. Summarize and analyze the test results and assess the feasibility of incorporating CNF in asphalt mixes as an additive.

1.5 Report Organization

This report is organized in the following order:

Chapter 1: Introduction – This chapter includes a background and a general summary of CNFs, electrospinning technique, and the organization of the study.

Chapter 2: Background – This chapter summarizes the literature review that focuses on the rheological, mechanical, and performance properties of asphalt mixes, polymer-modified binders, and non-polymer-modified binders. A literature review focusing on the development, advantages, production, and performance of asphalt binders and asphalt mixes containing different types of fibers is also presented in this chapter.

Chapter 3: Materials and Methods – This chapter describes the selection and collection of the materials, the production of CNF in the laboratory, and the modification of asphalt binder and mix. Also presented are the methodologies used for the laboratory characterization of the produced CNF, the neat and CNF-modified asphalt binders, and asphalt mixes.

Chapter 4: Results and Discussions – Evaluation results and analysis of the roughness, entanglement, average diameter, and tensile strength of the different CNFs produced are presented in this chapter. Also, the selection of the optimum solution and electrospinning parameters for CNF production is presented in this chapter. Analyses of the Izod impact strength test, RV, and BBS tests conducted on the different neat asphalt binders and CNF-modified binders are presented in this chapter. This chapter also analyzes the results obtained by conducting the HWT, SCB, and TSR tests on the asphalt mixes containing different amounts of CNF.

Chapter 5: Conclusions and Recommendations – Important findings of this study and the recommendations based on these findings are presented in this chapter.

2. BACKGROUND

Hot-mix asphalt (HMA) is the most used material for constructing roads and highways. Over 550 million tons of HMA are produced annually in the U.S. (Hansen and Copeland, 2017). In this process, the asphalt construction industry consumes over 24 million tons of asphalt binder annually. This amount accounts for over $12 billion in value (Williams et al., 2024). The production of asphalt binder is carried out by distilling crude oil in refineries. In recent decades, with environmental awareness and increased momentum for the application of renewable resources, a new generation of asphalt technologies was introduced. These technologies include novel materials and innovative methods to address environmental and economic challenges and enhance the quality of asphalt pavements. For example, the mechanical properties of asphalt binders were significantly improved by incorporating petroleum-based polymers. Modifying neat asphalt binders with polymers, such as styrene-butadiene rubber (SBR), styrene-butadiene-styrene (SBS), and ethylene vinyl acetate (EVA), are shown to improve their resistance to low-temperature cracking, permanent deformation, fatigue cracking, and moisture-induced damage (Yildirim, 2007). While beneficial, polymers used for producing polymer-modified asphalt binders (PMB) have a non-renewable origin and are more costly than non-polymer-modified binders (Toraldo and Mariani, 2014). As a result, the asphalt construction industry is susceptible to fluctuations in oil production and its cost, supply disruptions, or scarcity of resources. Several researchers have pursued the viability of using different additives in asphalt binders to reduce the need for polymers and petroleum-based binders. Consequently, plastics, elastomers, fibers, and other chemical additives have been considered and researched as asphalt binder modifiers (Daly, 2017). Ground tire rubber, polyphosphoric acid, waste cooking oil, extenders, synthetic fibers, mineral and synthetic fillers, oxidants, antioxidants, hydrocarbons, bio-fuel byproducts, lignin, animal-derived bio-binder, and their combinations as asphalt additives are among several alternative materials that have been studied (e.g., Ghabchi et al., 2021a, b; Ghabchi and Castro, 2022; Ghabchi, 2022; Ghabchi and Castro, 2021a, b; Kocak and Kutay, 2020; Yu et al., 2020; Sarkar et al., 2020; Hossain et al., 2020; Ameli et al., 2020; Li et al., 2020; Ziari et al., 2020; Fini et al., 2019; Daly, 2017; Sun et al., 2016; Wen et al., 2013). While these alternatives have been found promising to some extent, quality inconsistencies of the biomaterials, their incompatibilities with some of the chemicals found in additives and asphalt, inconsistent performance, lack of standard practice, and the energy needs for bio-binder production, along with the lack of performance records, are among factors limiting their use in asphalt pavement construction. Plant-based products are available in low-cost, sustainable, and environmentally friendly materials and have been proven to have significant potential for several applications. For example, soy protein, corn, and cellulose are used to produce effective and practical bonding agents (Airey and Mohammed, 2008). Cellulose is the most abundant natural bio-material and can be processed to produce fibers with tensile strength and elastic modulus values as high as 60 MPa and 3 GPa, respectively (Oishi et al., 2015). Therefore, if the feasibility and the benefits of its use in asphalt binder are proven, it will become a good candidate as an asphalt additive to improve the mechanical properties of asphalt mixes as an effective and environmentally sustainable solution. Additionally, nano-reinforced materials are shown to possess a high potential for improving the desirable engineering properties of traditional pavement materials both in terms of performance and potential applications (Khattak et al., 2011). These materials exhibit temperature sensitivity, high ductility, large surface area, and high strain resistance (Li et al., 2017). Different types and amounts of nanomaterials when incorporated into asphalt binder, namely carbon nanofibers (Yang et al., 2020; Khattak et al., 2012), carbon nanoparticles (Amirkhanian et al., 2011), carbon nanotubes (Sheng et al., 2020; Xin et al., 2020; Ziari et al., 2014), nano-clay (Hamedi et al., 2020; Ghanoon et al., 2020), nano ZnO (Su et al., 2020), and nano SiO_2 (Karnati et al., 2020; Shafabakhsh et al., 2020), have shown significant potential for improving the mechanical characteristics of asphalt binders and mixes. Therefore, using cellulose as CNF in asphalt binders and mixes was hypothesized to enhance their mechanical properties. Note that cellulose fibers have historically been used in stone matrix asphalt to prevent asphalt binder drain-down. However, the production of cellulose nanofibers and their application as an asphalt binder modifier has not been explored in the past. While polymer modification and the use of other additives derived from non-

renewable resources are practiced as a means for improving the mechanical properties of asphalt binders and mixes, there is a need to explore more sustainable, cost-effective, renewable, and environmentally friendly alternatives to polymers, which can improve the mechanical properties of asphalt binders and mixes while minimizing dependency on oil. In response to this need and given the abundance of cellulose, its cost-effectiveness, favorable mechanical properties, sustainability, environmental friendliness, and renewability, CNF was studied as a candidate additive to be incorporated into asphalt binders and mixes intending to improve their durability and mechanical properties.

Therefore, this study was undertaken to produce CNF in the laboratory and evaluate the effect of using CNF in asphalt binders and mixes on their performance and mechanical properties. For this purpose, an in-house-fabricated electrospinning device produced CNF in the laboratory. The electrospinning parameters were adjusted, and the effectiveness of the production technique in achieving consistent CNF was verified. The directional (horizontal and vertical) tensile strength of the lab-produced CNF was determined. In addition, the structure, orientation, geometry, and morphology of the lab-produced CNF were assessed by conducting SEM imaging.

Furthermore, post-processing of the SEM images helped determine the CNF diameter distribution. After the selection of the CNF for asphalt binder modification, Superpave asphalt binders, PG 58-28, PG 64-34, and PG 70-28, were blended with different amounts of CNF (0%, 0.3%, and 0.7% by the weight of binder) and mixed by a high-shear mixer. Asphalt binder-aggregate adhesion with granite, quartzite, and gravel and their moisture-induced damage potential were evaluated by conducting BBS tests on dry and moisture-conditioned specimens. To evaluate the impact of CNF incorporation in asphalt binder blends with different doses (0%, 0.2%, 0.3%, 0.5%, and 0.7%) on their fracture energies measured at low temperatures, an Izod impact test was implemented as an innovative adoption of an existing testing technique for asphalt binders. The effect of incorporating different amounts of CNF in different binder blends on their dynamic viscosity was characterized by conducting an RV test. Finally, Superpave asphalt mixes having a nominal maximum aggregate size (NMAS) of 12.5 mm were produced using a PG 58-28 asphalt binder, 20% reclaimed asphalt pavement (RAP), and 0%, 0.3%, and 0.7% CNF by the weight of the binder. The effect of incorporating CNF in mixes on their resistance to cracking, rutting, and moisture-induced damage was characterized by SCB, HWT, and TSR tests, respectively.

3. MATERIALS AND METHODS

3.1 Materials

3.1.1 Electrospun Cellulose Nanofibers

Fibers having a mean diameter in the range of micrometers to nanometers can be produced by application of the electrospinning technique, a cost-effective and efficient method for harvesting fibers from a wide variety of polymers (Aman Mohammadi et al., 2020; Tungprapa et al., 2007). Sketches of the static and rotating electrospinning setups used to produce CNFs in this study are shown in Figures 3.1a and 3.1b, respectively.

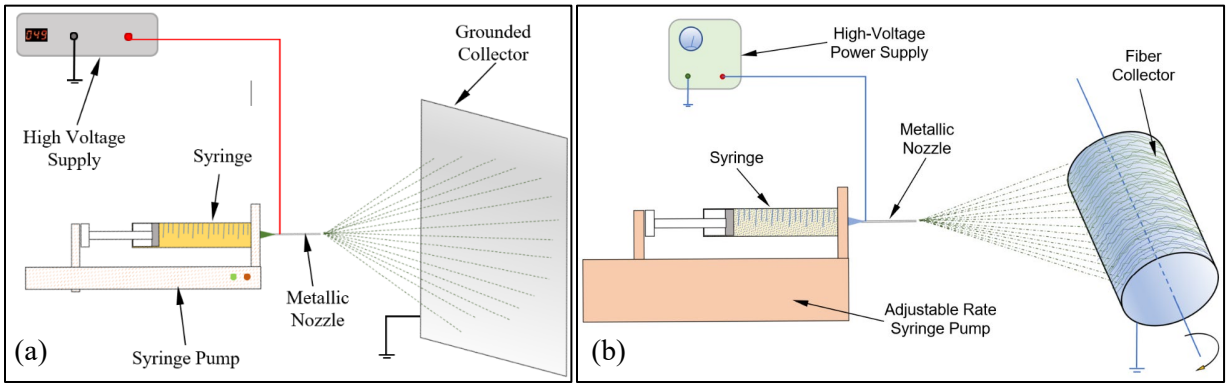

Figure 3.1 Schematic images of (a) static and (b) rotating electrospinning techniques

The principle behind the electrospinning technique, as shown in Figure 3.1, is the flow of a polymer solution out of the tip of a metallic needle, where a droplet forms under the influence of the surface tension of the electrospinning solution. A high electric charge is applied to the solution, developing repulsive electrostatic forces between polymer and solvent molecules to overcome the surface tension (Liu et al., 2019). A high electric charge difference between the tip of the nozzle and a grounded collector forms an electrohydrodynamic jet driven by electrostatic forces and deposits strands of fibers onto the grounded collector (Mehta et al., 2017; Tungprapa et al., 2007; Smit et al., 2005; Subbiah et al., 2005; Son et al., 2004).

As a cellulose derivative, cellulose acetate (CA) is used for various applications, including producing cellulose fibers. Therefore, this study used CA from Sigma Aldrich (Figure 3.2) to produce electrospun CNF in the laboratory. CA as a polysaccharide is an important cellulose ester obtained from the reaction of cellulose with acetic anhydride and acetic acid in the presence of sulfuric acid (Fischer et al., 2008). Up to two hydroxyl groups of each glucose ring in the cellulose structure undergo acetylation (Biswas et al., 2020). CA, with a molecular weight of 146 kg/mole and 1.31 degrees of acetylation, is soluble in acetone (Biswas et al., 2020). Due to the low boiling point of acetone, using a solution of CA and acetone for electrospinning is reported to lead to clogging of the nozzle's tip and interruption in the process (Tunggprapa et al., 2007). Therefore, different mixes of CA, acetone, acetic acid, and water were used in this study, as suggested by Han et al. (2008) and Son et al. (2004), to produce CNF in the laboratory. After reviewing the open literature and examining different electrospinning parameters—voltage, CA concentration, acetone-to-water proportions in the solution, and tip-to-collector distance—different solution and volumetric proportions were selected and applied in this study (Liu and Hsieh, 2002). The electrospinning solution was prepared by dissolving the required amounts of CA in the solvent described earlier using a magnetic stirrer at 50°C for 20 minutes and used after bringing it to room temperature. A syringe was filled with the solvent and placed inside a syringe pump (Figure 3.1) with a predetermined

discharge rate. The tip of the syringe was connected to one end of a small plastic tube while its other end was connected to a syringe needle used as a nozzle with an inner diameter of 1.6 mm. The metallic end of the nozzle was connected to high-voltage supplied by a transformer. Depending on the selected electrospinning technique, a rotating conductive drum or a stationary collection plate was utilized.

Electrospinning was conducted at room temperature and continued for 20 minutes (collection time). After completion of electrospinning, the sample weight was measured and recorded. Electrospun fibers and aluminum foil were kept in a desiccator for further evaluation. Figure 3.3 shows a photographic view of an electrospun CNF mat sample. Table 3.1 presents the compositions of the solutions used to produce CNF in the laboratory. Table 3.2 presents the electrospinning parameters and the solutions used to produce CNF in this study.

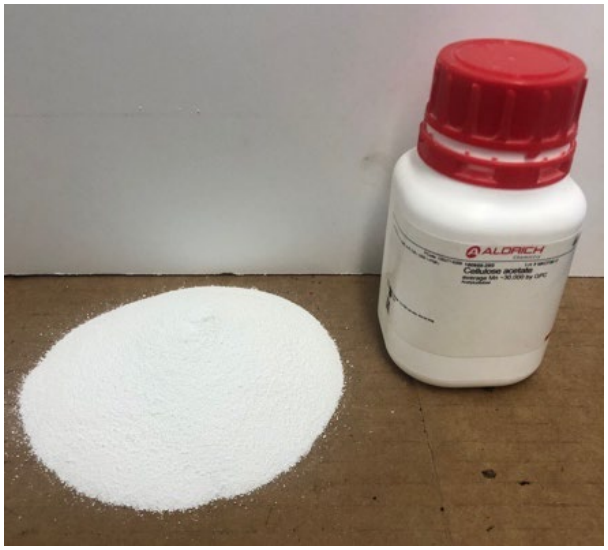

Figure 3.2 Cellulose acetate used for the production of the CNF

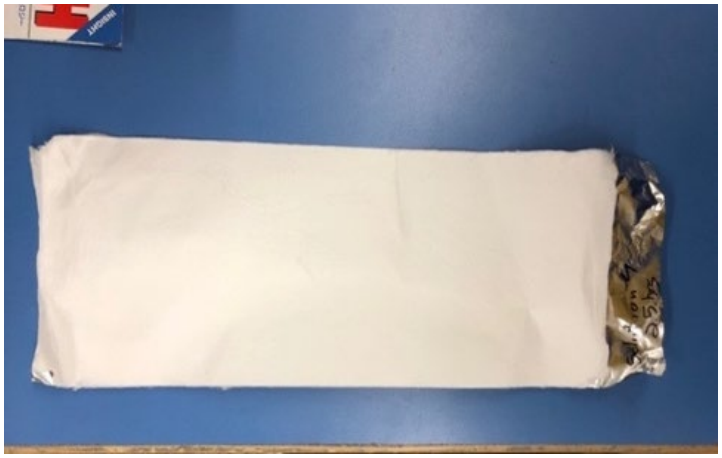

Figure 3.3 A photographic view of the produced CNF mat

Table 3.1 Electrospinning solutions' compositions

Solution Type	Solvent Type and Volumetric Ratio	CA Amount (% by weight)
1	Acetone (100%)	15
2	Acetic Acid (100%)	13
3	Acetic Acid (75%)/Water (25%)	17
4		13
5	Acetone (88%)/Water (12%)	17

Table 3.2 Initial electrospinning parameters used for preparing CNF samples

Sample No.	Solution Type and Voltage	Collection Time (minutes)	Discharge Rate (ml/min)	Tip-to-Collector Distance (cm)
1	**Solution 1** 15 kV	2	0.01	17
2		2		17
3		5		17
4		5		17
5		10		17
6		10		17
7		20		17
8		20		17
9		60		17
10		60		17
11	**Solution 2** 15 kV	2	0.01	17
12		2		17
13		5		17
14		5		17
15		10		17
16		10		17
17		20		17
18		20		17
19		60		17
20		60		17
21	**Solution 3** 15 kV	2	0.01	17
22		2		17
23		5		17
24		5		17
25		10		17
26		10		17
27		20		17
28		20		17
29		60		17
30		60		17
31	**Solution 4** 15 kV	2	0.01	17
32		2		17
33		5		17
34		5		17
35		10		17
36		10		17
37		20		17
38		20		17
39		60		17
40		60		17
41	**Solution 5** 15 kV	2	0.5 to 1.0	17
42		5		17
43		2		12.5
44		5		12.5
45		2		7.5
46		5		7.5

Conducting the electrospinning according to Table 3.2 and observations made during that stage led to exploring more combinations of electrospinning parameters to optimize them further. Table 3.3 presents the additional combinations of the electrospinning parameters to achieve CNF with better quality compared with the previous samples.

T**able 3.3** Adjusted electrospinning parameters used for preparing CNF samples

Sample No.	Solution Type	Collection Time (minutes)	Voltage (kV)	Discharge Rate (ml/min.)	Tip-to-Collector Distance (cm)
1.1	1	15	15	1	17
1.2		15	15		17
1.3		10	15		17
2.1	2	15	15	0.2	17
2.2		15	15		17
2.3		15	15		17
3.1	3	15	20	0.01	17
3.2		15	20		17
3.3		20	15		17
4.1	4	15	15	0.3	17
4.2		15	15		17
4.3		15	15		17
5.1	5	20	15	0.01	17
5.2		20	15		17
5.3		20	15		17

3.1.2 Asphalt Binder

Three different types of asphalt binders, PG 58-28, PG 64-34, and PG 70-28, were collected from a material supplier in Sioux City, IA. Asphalt binders were used to prepare samples for conducting the Izod impact, RV, and BBS tests. Collected asphalt binders were heated and poured into smaller cans for further evaluation (Figure 3.4). Adequate blending and dispersion of the CNF in asphalt binder is vital to obtaining a consistent quality. A composite material consisting of fibers can only exhibit improved mechanical properties when fibers are homogeneously dispersed in the material (Wang et al., 2017). As a result, a procedure was developed and followed, and the incorporation of CNF in asphalt binder resulted in a consistent dispersion of the CNF in binder blends. The CNF mat (Figure 3.3) was cut into pieces of 2-cm width each. The CNF ribs were then further cut to form 0.5-cm by 2.0-cm CNF staples. Finally, the required CNF concentrations were used to measure and spare a predetermined amount of CNF staples. The CNF staples were pulled to separate the yarns in a carding process and were gradually added according to the required weight to liquid asphalt binder in an oven at 165°C. The asphalt binder blend was continuously mixed inside the oven using an in-house-fabricated shear mixer consisting of a 50-mm-diameter steel spiral mixing arm attached to a drill inside an oven and operating at an approximately 1,000-rpm rotational speed. In this process, a mixing time of 1.5 hours was used for all CNF-asphalt binder blends. Mixing was carried out while the binder container was covered using an aluminum foil layer to minimize aging. Additionally, to maintain a consistent level of aging and oxidative hardening for all binder samples, the above heating and shear mixing procedure was followed for asphalt binders containing no additives.

Figure 3.4 A photographic view of an asphalt binder sample in a small can

3.1.3 Aggregates

Three types of aggregates—granite, quartzite, and gravel—were collected from quarries in Grant County, Minnehaha County, and Brookings County, respectively, in South Dakota. Local contractors widely use collected aggregates for city and interstate highway asphalt pavement construction projects. Both crushed and graded aggregates and large rocks with a minimum diameter of 300 mm were collected and stored in the laboratory for sample preparation and further evaluation.

3.1.4 Asphalt Mix

A Superpave asphalt mix designed following AASHTO M 323 (AASHTO, 2017) standard specification and AASHTO R 35 (AASHTO, 2017) standard practice was evaluated in this study. The asphalt mix contained a PG 58-28 asphalt binder and 20% RAP by the weight of aggregates. The mix aggregates mainly consisted of granite, quartzite, and gravel from local quarries with a combined nominal maximum aggregate size (NMAS) of 12.5 mm. Volumetric parameters of the asphalt mix are presented in Table 3.4, which shows that the optimum binder content was 5.8%, consisting of 4.8% virgin PG 58-28 binder and 1% replaced by RAP binder. Recorded void in mineral aggregates (VMA), voids filled with asphalt (VFA), and dust proportion (DP) values were found to be 14.5%, 72.4%, and 1.0, respectively, all within the ranges recommended by AASHTO M 323 (AASHTO, 2017). The combined aggregate particle size distribution used in the asphalt mix is shown in Figure 3.5.

Table 3.4 Important volumetric properties of asphalt mix

Asphalt Binder Grade	Virgin Asphalt Binder (%)	Replaced Asphalt Binder (%)	RAP (%)	Voids in Mineral Aggregates (Required: >14%)	Voids Filled with Asphalt (%) (Required: 70% – 80%)	Dust Proportion (Required: 0.6 – 1.2)
PG 58-28	4.8%	1.0%	20%	14.5%	72.4%	1.0

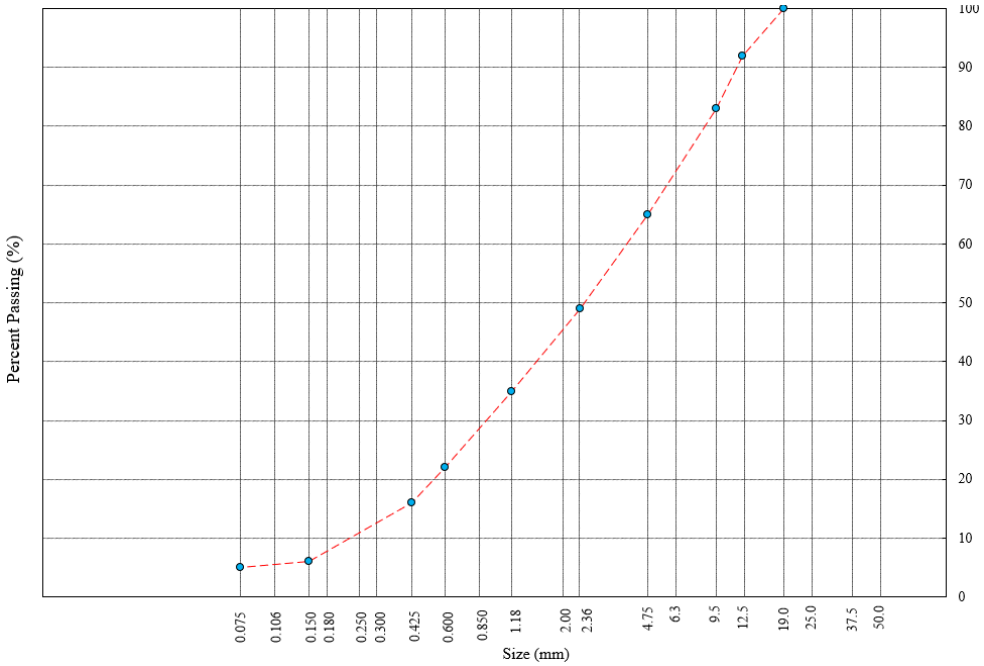

Figure 3.5 Aggregate gradation of the asphalt mix

3.2 Test Methods

3.2.1 Scanning Electron Microscopy

To study the structure and morphology of the produced electrospun CNF, a scanning electron microscopy (SEM) imaging technique was applied. In the SEM technique, a focused beam of electrons is applied to scan the surface of the specimen to generate a high-resolution image of the sample under study. For this purpose, Hitachi S-3400N SEM equipment was employed to study the structure and morphology of the CNF samples coated by a thin conductive layer. For this purpose, the sample was coated with a layer of gold having a 10-nm thickness.

3.2.2 Tensile Strength Test of Fibers

Produced CNF samples were prepared and tested to determine their tensile strength in an MTS® Insight 5 loading frame. Since the produced CNF has a nonwoven structure and due to its small dimensions, testing individual fibers was not practical. To ensure the consistency of the test specimens and to make it possible to measure the tensile strength of approximately the same cross-sectional area of the CNFs at each sample, the test specimens having constant weights and constant dimensions were used. For this purpose, CNF samples produced on a static aluminum foil collector were used. The 36 cm x 12 cm CNF mat was carefully detached from the aluminum foil and returned to it as a loose mat. The aluminum foil and CNF mat were then folded several times in different directions to form an 8-layer mat. The final sample was cut from its long ends to obtain a sample with a length of 16 cm and a width of 2 cm. The prepared sample was weighed using a lab balance with a 0.001 g resolution. The samples' measured weights ensure the same concentration of CNF in all samples with the exact dimensions. Finally, the sample was placed in the loading frame and clamped equally from both ends, leaving an 8-cm sample length for testing. The test specimen was subjected to tensile loading with an actuator displacement rate of 2 mm/minute. Loads were measured using a 5-kN load cell and were recorded using a data acquisition system operated at a frequency of 50 Hz. Collected load and displacement data were analyzed to calculate the tensile strength.

Since the tested CNF mat had a nonwoven structure, tensile strength tests were conducted in two perpendicular directions (X and Y) to capture any planar anisotropy in electrospun CNF.

3.2.3 Rotational Viscometer (RV) Test

Adding CNF to an asphalt binder can result in a change in its viscosity. Proper viscosity is needed to achieve adequate aggregate coating during mixing and reasonable workability during construction. To determine the effect of incorporating CNF in asphalt binders on their dynamic viscosity, rotational viscometer (RV) tests were conducted using a Brookfield RV on unaged asphalt binder blends per AASHTO T 316 (AASHTO, 2019) standard method. The RV tests were conducted on asphalt binders PG 58-28, PG 64-34, and PG 70-28, each blended with CNF at concentrations of 0%, 0.3%, and 0.7% by the weight of the binder. Asphalt binder blends prepared using the procedure described in section 3.1.2 were used for conducting the RV tests.

3.2.4 Izod Pendulum Impact Resistance Test

The Izod pendulum impact resistance test is used following ASTM D256-10 (ASTM, 2018) for determining the fracture energy absorbed by the plastic materials and polymers due to the impact of a standardized pendulum hammer in an Izod impact machine (ASTM, 2018). In this method, if a notched sample is used, the sample is more likely to undergo a brittle fracture (ASTM, 2018). The capability of the Izod pendulum test in capturing the material's fracture energy and its unique testing speed have made it an ideal candidate to quickly evaluate the fracture energy of asphalt binders as an innovative adoption of an existing approach. Therefore, the Izod pendulum impact test was used to test asphalt binder samples to determine the effect of different asphalt binders containing different amounts of CNF on their brittleness at low temperatures. Additionally, an asphalt sample preparation method for the Izod test was developed and used for testing. Theoretically, a high absorbed fracture energy indicates a high ductility in asphalt binder, which is expected to result in a higher resistance to cracking. Therefore, applying this method is expected to spot vitiations in binders' resistance to cracking quickly and easily. Sample preparation and testing of several binders can be conducted altogether in a single day. Also, after validation of its results by other laboratory tests and calibration by field observations, this method is expected to correlate with the mixes' resistance to cracking. More research is underway to achieve this objective, but this is not within the scope of the current study. To prepare the asphalt binder specimen (test beam), a modular aluminum mold was designed and fabricated in the laboratory (Figure 3.6a). The fabricated mold was designed to cast test beams with 12 mm x 12 mm x 64 mm dimensions. Plastic strips 0.05-mm thick were cut and placed inside the test beam mold to facilitate detaching the specimen from the mold. A small amount of petroleum-based grease was applied to the interior faces of two sides and base pieces of the mold to hold the plastic strips in place. The mold was assembled, and four 19-mm foldback metal binder clips were used to hold the mold pieces together (Figure 3.6b). Liquid asphalt binder blend was carefully poured from one end and moved toward the other end inside the assembled mold until the mold was slightly overfilled. After cooling at room temperature for approximately one hour, the exposed face of the specimen was trimmed using a hot blade. The trimmed sample in the mold was kept in a freezer at -14°C for two hours. The binder clips were then removed, and the mold was disassembled carefully to obtain the test beam (Figure 3.6c). A notch with a 2.3-mm depth was created in the midspan of the test beam by a hot blade using two aluminum templates fabricated in the lab (Figure 3.6d). The prepared test beam was returned to the freezer and kept at -14°C for two hours before testing.

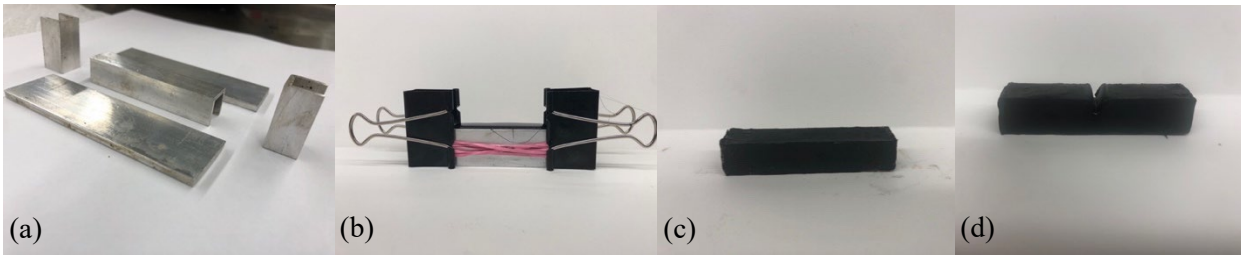

Figure 3.6 Izod test beam preparation (a) pieces of fabricated aluminum mold; (b) assembled mold; (c) test beam; (d) test beam with notch

The pendulum, with a mass of 450 g in standardized Izod test equipment, was raised and locked in place (Figure 3.7). A digital angle logger attached to the equipment was used to record the angle pendulum at rest in the vertical direction. The test specimen was then removed from the freezer and quickly clamped in the vise so that the notched side faced the impact direction and the notch line was at the same level as the top of the vise. The pendulum was released, and the digital angle logger recorded its maximum angle with the vertical direction after breaking the sample. Note that clamping the specimen in the vise and releasing the pendulum was carried out within 30 seconds after removing it from the environmental chamber. Total corrected fracture energy was determined based on the recorded angles, the pendulum mass, and the moving assembly from Equation 3.1. The required corrections were applied according to the manufacturer's instructions to account for energy loss due to windage and friction. The corrected fracture energy was divided into a cross-section of the notched area to determine the fracture energy absorbed by the unit cross-sectional area of the asphalt specimen (Equation 3.2).

$$E_{cor.} = MgL\,(\cos\beta - \cos\alpha) - E_{TC} \tag{3.1}$$

where $E_{cor.}$ = corrected fracture energy absorbed by the specimen (J); M = mass of pendulum determined following ASTM D256 (kg); g = gravitational acceleration (9.80665 m/s^2); L = distance from the fulcrum to center of gravity of pendulum (m); β = maximum angle of pendulum position after impact from its rest position; α = maximum angle of pendulum position before impact from its rest position; E_{TC} = total energy loss correction for a given breaking energy (J), as described in ASTM D256.

$$E_{abs.} = E_{cor.}/A \tag{3.2}$$

where, $E_{abs.}$ = corrected fracture energy absorbed by the unit cross-sectional area of the specimen (J/m^2); and A = area of the notched cross-section pf the specimen (m^2). At least 15 separate Izod impact tests were conducted for each binder blend.

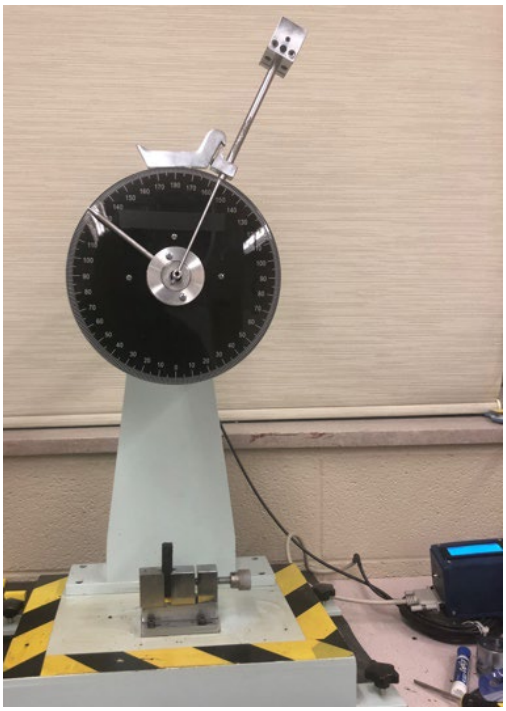

Figure 3.7 Izod impact test equipment used for conducting tests on the asphalt specimens

3.2.5 Binder Bond Strength (BBS) Test

The BBS tests were conducted following the AASHTO T 361 standard method (AASHTO, 2016) on asphalt binder-aggregate systems. The BBS is a quick and reliable test method for evaluating the quality of binder-aggregate adhesion by measuring pull-off strength (POS) utilizing a pneumatic adhesion tensile testing instrument, PATTI (Figure 3.8a). The BBS test was used to evaluate the effect of CNF in different asphalt binders on their adhesion with different aggregate types before and after moisture conditioning. The collected rocks were prepared by cutting them into flat tiles to prepare the BBS test specimens. The rock tile surfaces were wet-polished using a grinder with a 1,500-grit diamond polishing pad. Polished aggregate tiles were cleaned several times using a brush sample while submerged in distilled water to remove dust. After drying the cleaned samples at room temperature, their surfaces were cleaned with acetone. The rock samples and pull stubs, which had a diameter of 25.4 mm, were kept in an oven overnight at 60°C to remove moisture. The hot liquid asphalt binder blend was placed in the center of the pull stub's surface and carefully spread using a hot spatula to form a consistent binder coating while slightly overfilling the pull stub's recess. The pull stub was then pushed and attached to the aggregate (Figure 3.8b). Excess asphalt binder squeezed from the bottom of the pull stub was cleaned using a heated utility blade. The specimens prepared for testing in dry conditions were kept in an environmental chamber at 25°C for 24 hours before testing. The binder-aggregate specimens were kept at 25°C for two hours, and then kept in the water at 25°C for 48 hours. Samples were moved inside an environmental chamber and kept at -18°C for 16 hours. Samples were transferred to a water bath and kept at 25°C for another four hours before testing. The BBS tests on moisture-conditioned samples were conducted while samples were kept in the water at a 25°C temperature to alleviate the possibility of erroneous POS measurements due to the formation of negative capillary pressure under the pull stub. The PATTI device was then connected to a compressed air supply, providing a pressure of 690 kPa. The pull-off piston was connected to PATTI, and data recording software was initiated. The correct types of piston and pull stub diameters were selected in the software, and the piston was fixed on the pull stub. The pressure flow button was pushed on the device, which resulted in the pneumatic piston being pushed and the pull stub being detached from the aggregate. The POS value of the tested specimen was obtained and recorded using PATTI software.

Also, a photograph of each failure surface was taken, and the failure mechanisms—cohesive and adhesive—were noted. The image was further analyzed to calculate the extent of the cohesive and adhesive failures by reporting the percentage area of samples that failed in cohesive or adhesive modes. At least 15 separate BBS tests were conducted, and POS measurements were recorded for each asphalt binder-aggregate system in dry conditions and after moisture-conditioning for a total of 270 BBS tests.

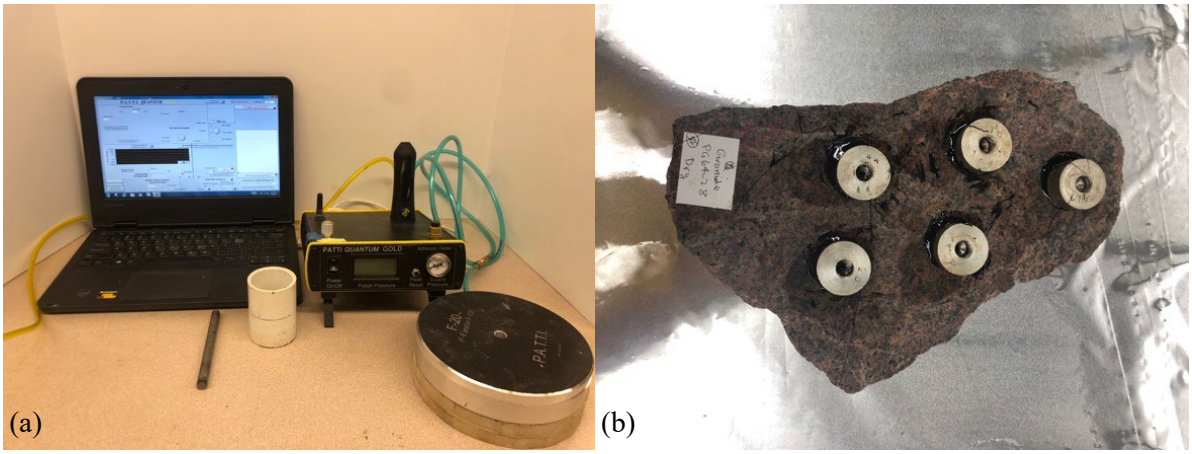

Figure 3.8 BBS test (a) PATTI test device and components, and (b) pull-off test specimen

3.2.6 Semi Circular Bend (SCB) Test

The SCB tests were performed to evaluate the effect of incorporating CNF in asphalt binder on the resistance of asphalt mixes to cracking. The SCB tests were conducted on asphalt mixes containing different CNF amounts (0%, 0.3%, and 0.7% by the weight of asphalt binder in the mix) using an asphalt mix performance tester (AMPT) according to ASTM D8044-16 standard method (ASTM, 2016). The SCB specimens were compacted in a Superpave gyratory compactor (SGC). For this purpose, the SGC was operated in height mode to compact cylindrical samples having a 150-mm diameter and 120-mm height (Figure 3.9a). Necessary adjustments were made to sample weight to obtain final SCB samples with 7.0% ± 0.5% air voids. Compacted cylindrical specimens were saw-cut into samples with a 57-mm thickness (Figure 3.9b). A tile saw was used to cut the 57-mm-height cylindrical samples diagonally to obtain semicircular samples. A precision table saw was used to cut 25.4, 31.8, and 38.1 mm-depth notches in the midspan of the semicircular samples (Figure 3.9c). After preparing the samples, their air voids were controlled by volumetric tests according to AASHTO T 166 (AASHTO, 2016) and AASHTO T 209 (AASHTO, 2020). The dry SCB specimens were kept at 25°C inside AMPT's environmental chamber and tested in a 3-point jig under a monotonic load applied at a rate of 0.5 mm/min to the midspan of the sample until failure (Figure 3.9d). Load and deformation data were recorded to determine the critical strain energy release rate (J_c) from Equation 3.3.

$$J_c = \frac{-1}{b}\left(\frac{dU}{da}\right) \tag{3.3}$$

where, J_c = critical strain energy release rate (kJ/m^2); b = sample thickness (m); a = notch depth (m); U = strain energy to failure (kJ); and dU/da = change of strain energy with notch depth (kJ/m). The trapezoidal method for numerical integration up to peak load was used to calculate U values from the collected load-deformation data. The value of dU/da was determined by calculating the slope of the linear regression model developed between the strain energy to failure (U) and notch depths (a). Asphalt mixes with a higher J_c value exhibit better resistance to fatigue cracking (Kim et al., 2012).

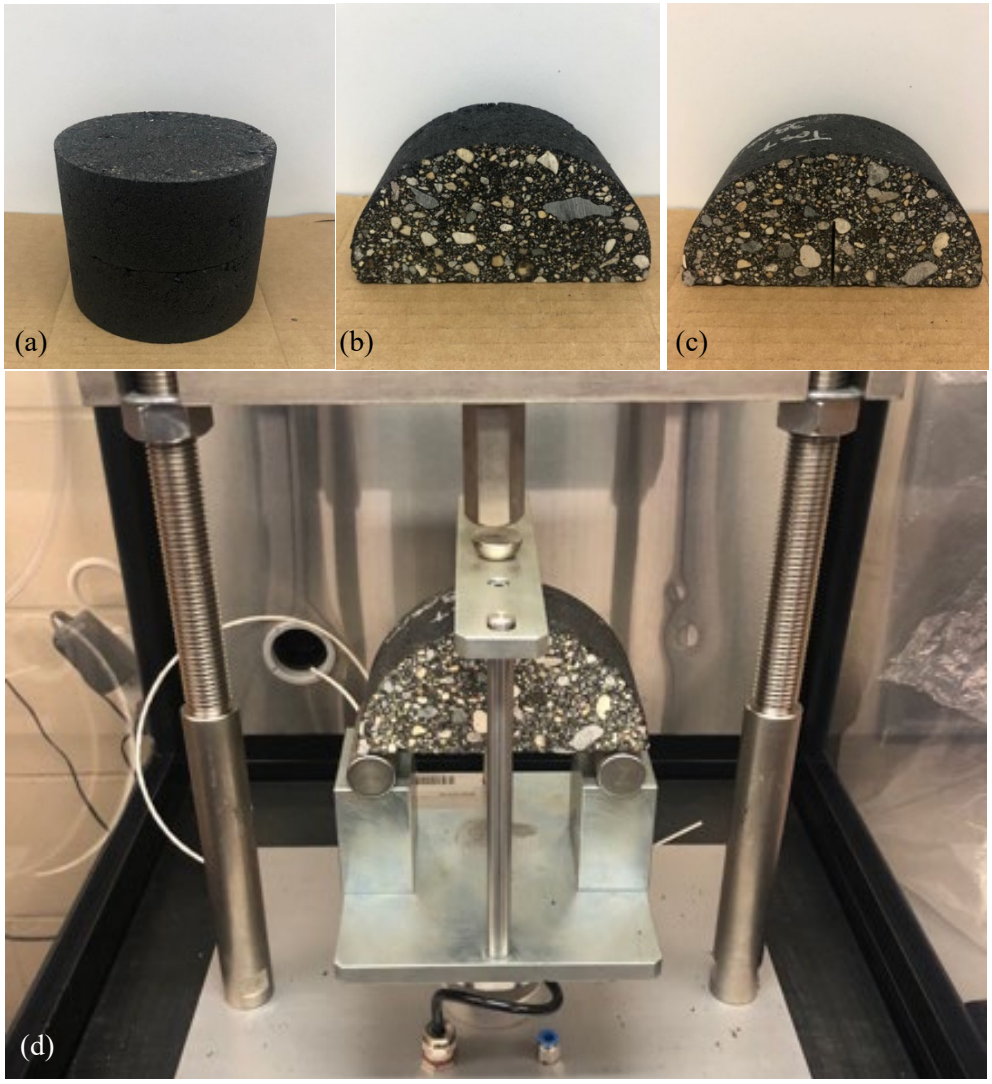

Figure 3.9 Conducting the SCB test (a) SGC-compacted cylindrical asphalt sample; (b) half-cylinder sample; (c) SCB sample with a mid-span notch, and (d) SCB test in progress

3.2.7 Hamburg Wheel Tracking (HWT) Test

Hamburg wheel tracking (HWT) tests, according to the AASHTO T 324 standard test method (AASHTO, 2019), were conducted on asphalt mixes to evaluate the effect of incorporating different amounts of CNF in the binders used in the mixes (0%, 0.3%, and 0.7% by the weight of asphalt binder) on their rutting and moisture-induced damage potentials. For this purpose, cylindrical HWT specimens 150 mm in diameter and 60 mm in height were compacted in an SGC operated in height mode (Figure 3.10a). Volumetric tests according to AASHTO T 166 (AASHTO, 2016) were conducted on compacted samples, and their air voids were determined. Necessary adjustments were made to the weights of the loose mix to obtain SGC-compacted cylindrical samples with 7.0% ± 0.5% air voids. At least four specimens for each mix with air voids of 7.0% ± 0.5% were compacted. A small segment was saw-cut from each cylindrical specimen to make them fit into the HWT mold (Figure 3.10b). A total of 12 specimens (3 mixes x 4 specimens each) within the target air voids range were compacted. A double-wheel standard tracker from Troxler was used to conduct the HWT tests (Figure 3.10c). First, samples were fit into special plastic molds and fixed in the device as instructed by its manufacturer. The procedure for controlling the HWT device was then initiated, important test parameters were entered, and the test started. The equipment water tank was filled

automatically, and the water temperature was set and maintained at 50°C. After reaching the thermal equilibrium, a pair of steel wheels, each with a 203-mm diameter, a 22.9-mm width, and a load of 705 N, were lowered automatically to touch the surface of the specimens. Submerged specimens were then subjected to 20,000 wheel passes through a cyclic loading action with a frequency of 53 ± 2 passes per minute. Wheel-pass numbers and deformation values measured at 11 equally spaced points on the sample were recorded and plotted. This plot was later utilized to determine the maximum permanent deformation and stripping inflection point (SIP), which represent the resistance of a mix to rutting and moisture-induced damage.

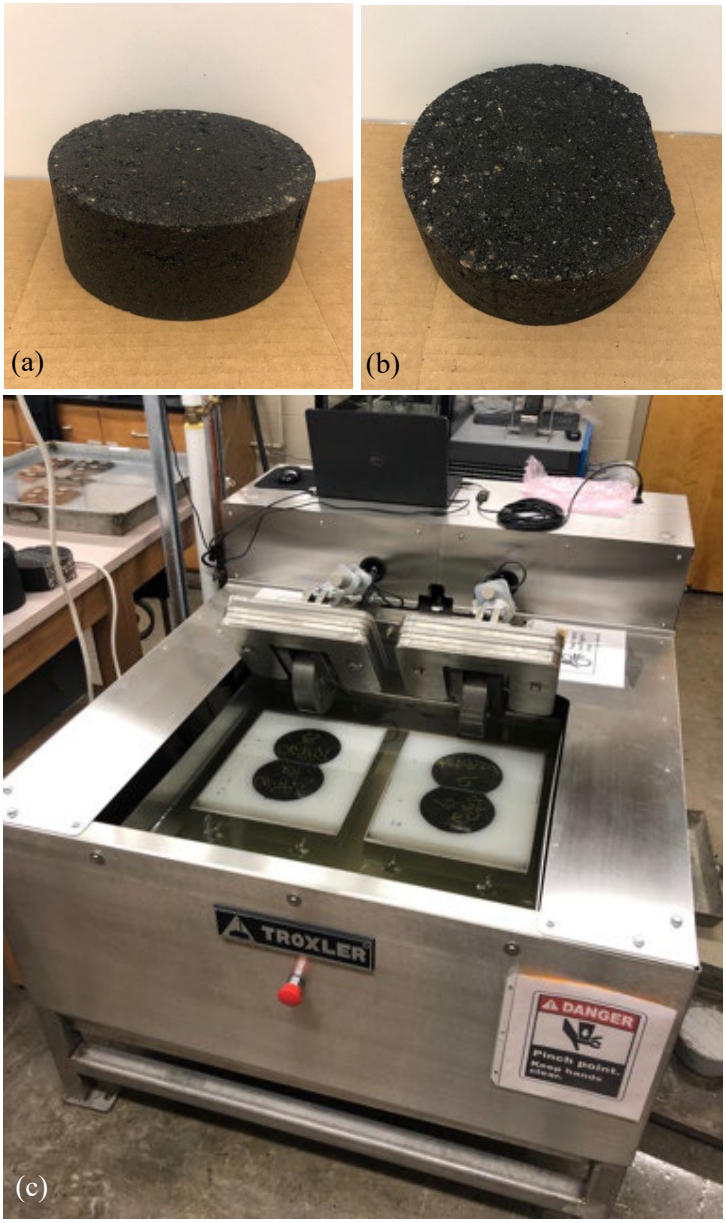

Figure 3.10 BBS test (a) PATTI test device and components, and (b) pull-off test

3.2.8 Tensile Strength Ratio (TSR) Test

Tensile strength ratio (TSR) tests were conducted on asphalt mixes following AASHTO T 283 (AASHTO, 2014) to evaluate the effect of incorporating CNF in asphalt mixes on their moisture-induced damage potential. Specimens for TSR tests were prepared in the laboratory using an SGC operated at height mode. At least eight cylindrical samples from each mix having a height and diameter of 95 and 150 mm, respectively, with target air voids of 7.0% ± 0.5%, were compacted. Compacted samples were divided into dry and moisture-conditioned subsets, each with four samples with equal average air voids. The dry subset was kept at 25°C in an environmental chamber. The other subset was vacuum saturated between 70% and 80% saturation, each sealed in an air-tight bag with 10 mL of water and kept in a freezer at -18°C for 16 hours. Afterward, the samples were placed in a water bath at 60° ± 1°C for 24 hours. They were kept in a water tank with a constant temperature of 25°C for two hours before testing.

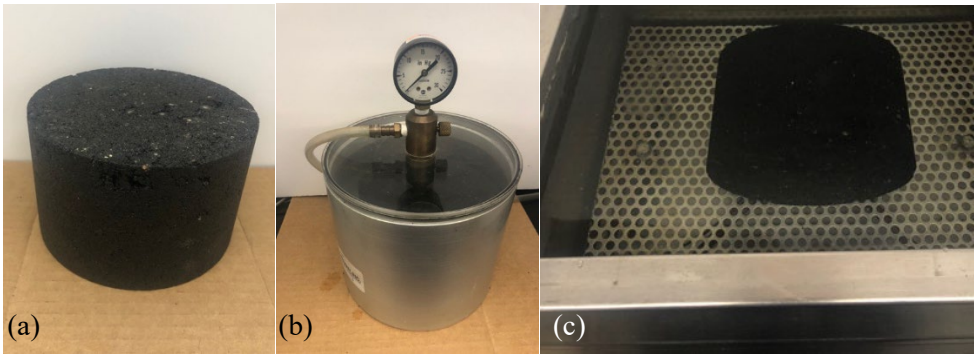

Figure 3.11 Sample preparation for TSR test (a) an SGC-compacted specimen, (b) vacuum-saturation chamber, and (c) moisture-conditioning an asphalt specimen in the water bath

An MTS loading frame with an indirect tension jig was used to test the specimens at 25°C by applying a load at a rate of 50 mm/min along the diameter of the sample until failure (Figure 3.12). The recorded peak load at failure was used to determine the indirect tensile strength of each specimen using Equation 3.4.

$$S_t = \frac{2000\,P}{\pi\,t\,D} \tag{3.4}$$

where, S_t = tensile strength (kPa); P = peak load at failure (N); t = specimen thickness (mm); and D = specimen diameter (mm). The ratio of the average tensile strength of the moisture-conditioned samples (ITS_{Wet}) to that of unconditioned samples (ITS_{Dry}) was reported as the TSR value of that mix (Equation 3.5).

$$TSR = ITS_{Wet}/ITS_{Dry} \tag{3.5}$$

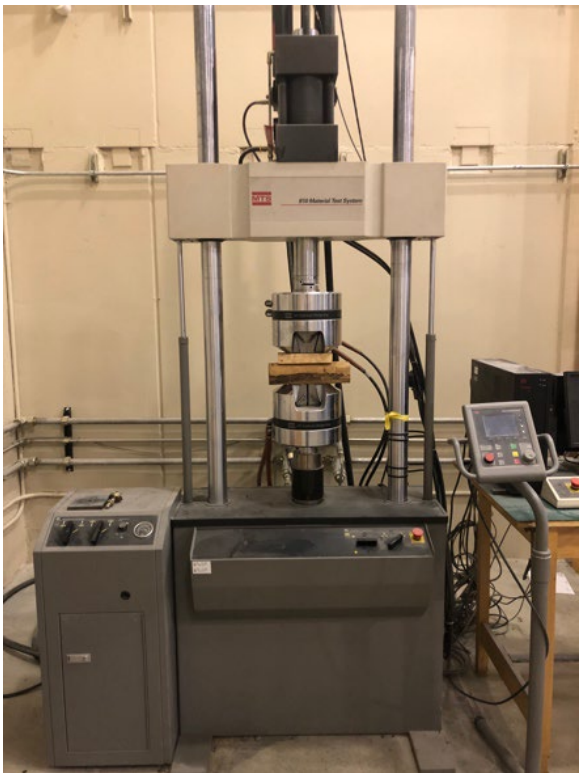

Figure 3.12 MTS® 810 loading frame used to conduct the TSR test

4. RESULTS AND DISCUSSION

4.1 Results of the Tests Conducted on CNF

4.1.1 Visual Inspection of the CNF Produced using Different Techniques

As discussed earlier, two electrospinning techniques were applied to produce the CNFs in the laboratory, namely rotating and static methods. In addition, five different types of electrospinning solutions (Table 3.1) were used to explore the most suitable combination of chemicals for the optimized CNFs. Figures 4.1, 4.2, 4.3, 4.4, and 4.5 depict photographic views of the CNFs produced using solutions 1, 2, 3, 4, and 5, respectively, and applying the rotating electrospinning technique. Visual inspection of fibers shown in these pictures revealed major differences in the formation and structure of each specimen, depending on the type of electrospinning solutions used. The visual inspection findings of the produced fibers in this category are summarized and presented in Table 4.1.

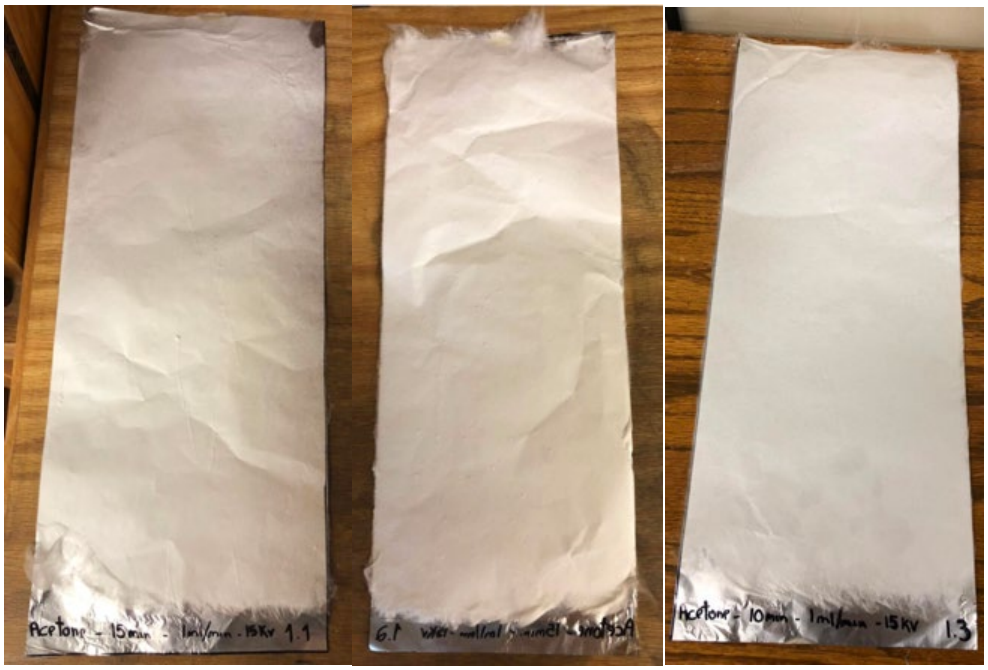

Figure 4.1 Photographic views of CNFs produced using solution 1 and rotating electrospinning technique

Figure 4.2 Photographic views of CNFs produced using solution 2 and rotating electrospinning technique

Figure 4.3 Photographic views of CNFs produced using solution 3 and rotating electrospinning technique

Figure 4.4 Photographic views of CNFs produced using solution 4 and rotating electrospinning technique

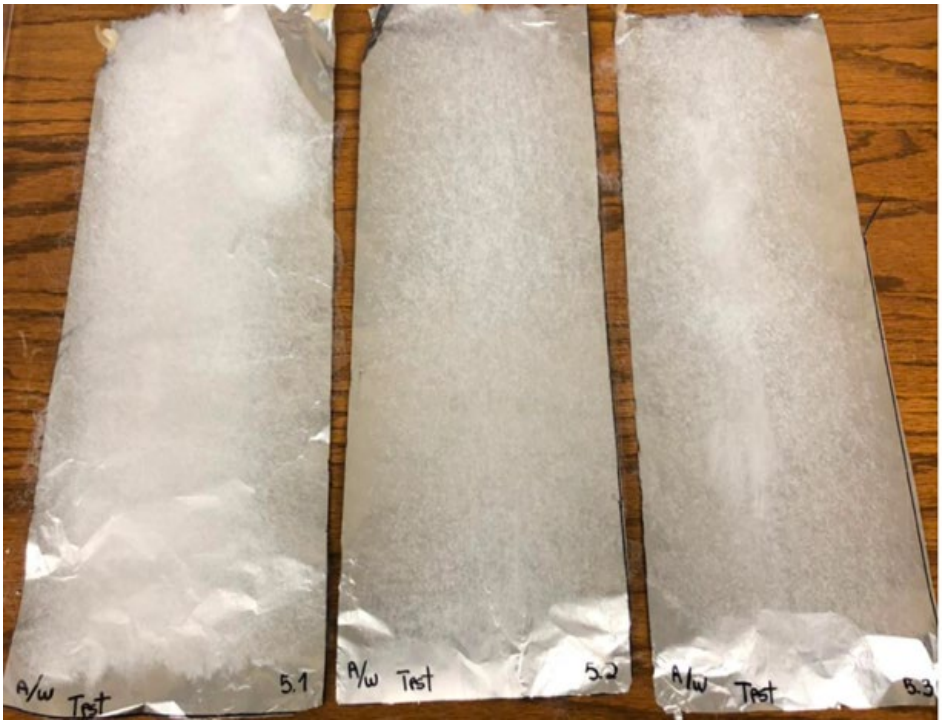

Figure 4.5 Photographic views of CNFs produced using solution 5 and rotating electrospinning technique

Table 4.1 Key observations made on the CNFs produced using different solutions and rotating technique

Solution Type	Key Observations
Solution 1 (CA/Acetone)	- The produced CNFs were dense and evenly spread on the collector plate. - It appeared to have a high thickness. - During the production, a few problems were observed. The solution solidified at the tip of the needle, slowing down the production of CNF. The high evaporation rate of acetone contributed to this problem.
Solution 2 (CA/Acetic Acid)	- The produced CNFs were not dense; only a thin layer of CNF was observed. - The CNFs were evenly spread on the collector plate. - The amount of CNFs produced seemed to be less when compared to other solutions.
Solution 3 (CA/Acetic Acid/Water)	- The produced CNFs were not dense; only a thin layer was overserved. - The solution behaved similarly to solution 2, producing less CNF when compared with others. - The main difference between the CNFs produced using solutions 2 and 3 is that the produced CNFs from solution 3 are not evenly spread on the collection plate. The CNFs are concentrated in the center from the top to the bottom of the collector plate.
Solution 4 (CA/Acetic Acid/Acetone)	- The produced CNFs were dense and evenly spread on the collector plate. - It is very similar to the produced CNF using solution 1. However, the produced CNF using solution 4 appears to have a smaller thickness. - The high evaporation rate of acetone was an issue, causing the solution to solidify at the tip of the needle, slowing the process.
Solution 5 (CA/Acetone/Water)	- The produced CNFs were visually inconsistent; all samples looked different. - A few produced CNFs were denser than the others. - A few produced CNFs were spread on the center from top to bottom, while others were evenly spread on the collector plate. - The thickness of the produced CNF was higher than the others. A 3D-like structure was observed. - The evaporation rate of acetone was a problem. The tip of the needle gets blocked due to the evaporation of acetone.

From Table 4.1 and based on visual inspection, structure, production repeatability, and the consistency of the produced CNF, solution 1 and 4 were identified as the candidates for the asphalt binder modification. The process of CNF production with solution 1 and solution 4 showed the minimum issues related to the high acetone evaporation. The final product of these two solutions showed a higher yield, density, and thickness when compared with the other fibers that were produced. However, additional laboratory tests were carried out to evaluate the produced fibers further and choose the optimum solution and technique.

Figures 4.6, 4.7, 4.8, 4.9, and 4.10 depict photographic views of the CNFs produced using solutions 1, 2, 3, 4, and 5, respectively, and applying the static electrospinning technique. Visual inspection of fibers shown in these pictures revealed major differences in the formation and structure of each specimen, depending on the type of electrospinning solutions used. Findings of the visual inspection of the produced fibers in this category are summarized and presented in Table 4.2.

Figure 4.6 Photographic views of CNFs produced using solution 1 and static electrospinning technique

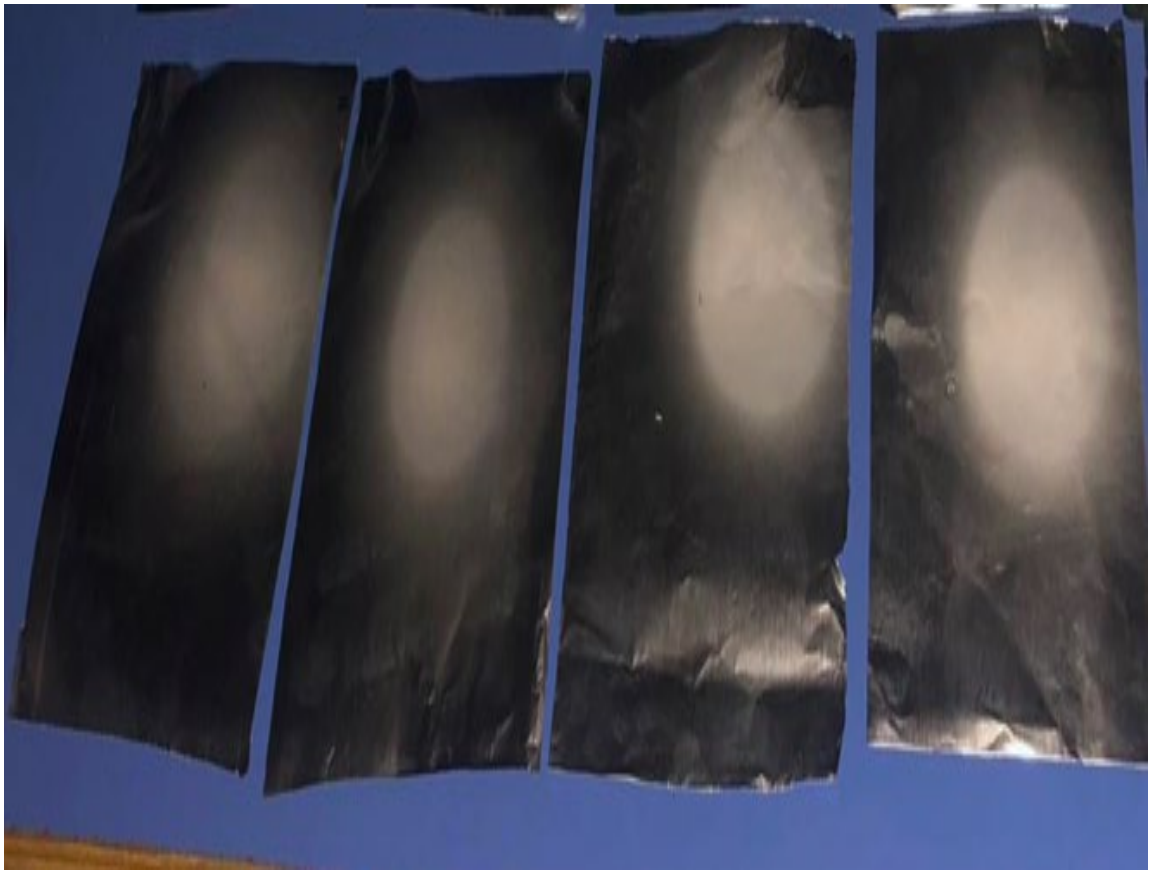

Figure 4.7 Photographic views of CNFs produced using solution 2 and static electrospinning technique

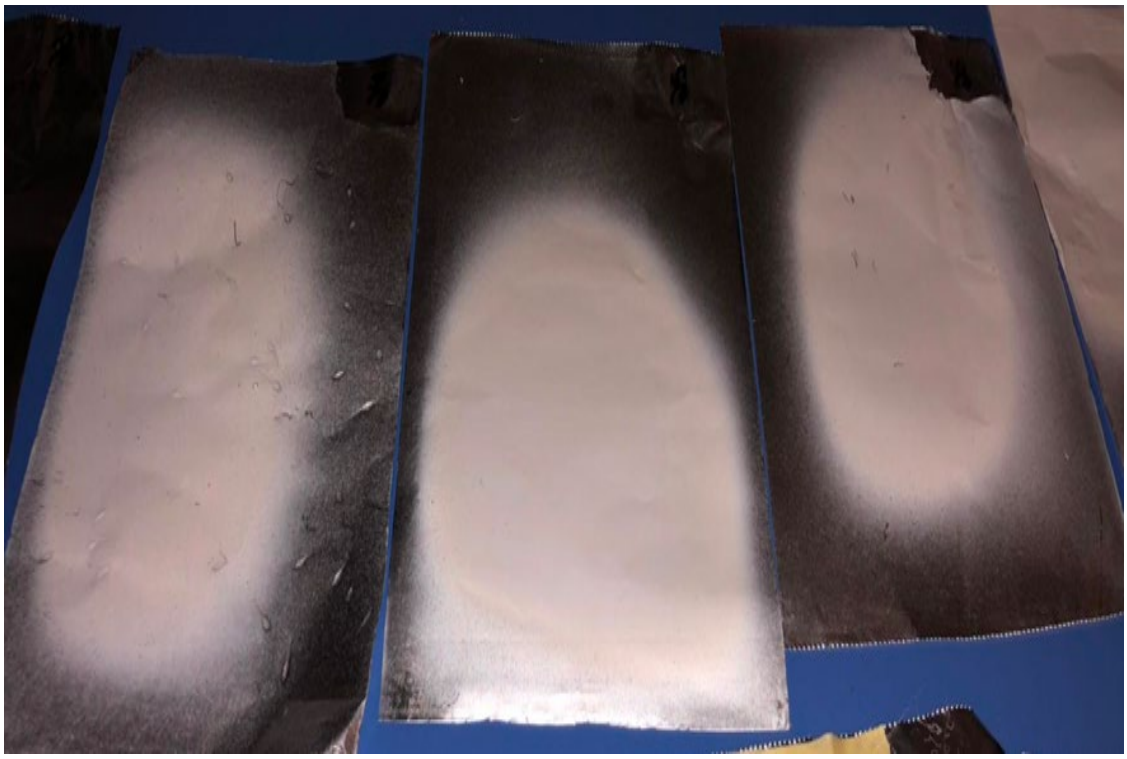

Figure 4.8 Photographic views of CNFs produced using solution 3 and static electrospinning technique

Figure 4.9 Photographic views of CNFs produced using solution 4 and static electrospinning technique

Figure 4.10 Photographic views of CNFs produced using solution 5 and static electrospinning technique

Table 4.2 Key observations made on the CNFs produced using different solutions and static technique

Solution Type	Key Observations
Solution 1 (CA/Acetone)	- The produced CNFs were dense and concentrated at the center of the collector plate. - It appeared to have a high thickness. - The solution solidified at the tip of the needle, slowing down the production of CNF. The high evaporation rate of acetone caused the problem.
Solution 2 (CA/Acetic Acid)	- The produced CNFs were not dense; only a thin layer of CNF was observed. - The thickness of the CNF mat was low. - The CNFs were concentrated at the center of the collector plate in a small area. - The amount of CNF produced seemed to be less when compared with other solutions.
Solution 3 (CA/Acetic Acid/Water)	- The produced CNFs were concentrated at the center of the collector plate. - The density and thickness of the produced CNFs were average compared with other solutions. - The density was similar to solution 1, but the thickness was similar to solution 2. - The solution behaved similarly to solution 2, producing fewer CNFs when compared with others. - The solution's viscosity was low, resulting in some droplets of the solution falling on the collector without spinning.
Solution 4 (CA/Acetic Acid/Acetone)	- The produced CNFs were dense and evenly spread on the collector plate. - Very similar to the produced CNFs using solution 1 with comparable thickness and density. - The high evaporation rate of acetone was an issue, causing the solution to solidify at the tip of the needle, slowing the process.
Solution 5 (CA/Acetone/Water)	- The produced CNFs were fluffy and fibrous. - The produced samples were more or less inconsistent in shape and structure. - The produced CNFs were concentrated at the center of the collector plate. - The thickness of the produced CNF was higher than the others. A 3D-like structure was observed. - The evaporation rate of acetone was a problem. The tip of the needle gets blocked due to the evaporation of acetone.

From Table 4.2 and based on visual inspection, structure, production repeatability, and the consistency of the produced CNF, solutions 1, 4, and 5 were identified as potential candidates for the asphalt binder modification. The process of CNF production with solutions 1, 4, and 5 showed the minimum issues related to the high acetone evaporation. The final product of these solutions showed a higher yield, density, and thickness when compared with the other fibers that were produced. Comparing the structures of the CNF fibers produced using these solutions revealed that CNFs produced through the static spinning of solution 5 have a more fibrous and less mat-like structure, which may improve its dispersion in asphalt binder. However, additional laboratory tests were carried out to evaluate the produced fibers further and choose the optimum electrospinning solution and technique.

4.1.2 Scanning Electron Microscopy (SEM)

The SEM tests were performed to gain important information regarding the structure and morphology of the laboratory-produced electrospun CNFs. Figures 4.11, 4.12, 4.13, 4.14, and 4.15 show SEM micrographs of the CNF matrices produced using solutions 1, 2, 3, 4, and 5, respectively.
From Figure 4.11, it was observed that the CNF filaments produced using solution 1 had a random orientation and did not follow any directional pattern, and they were densely positioned to each other. However, a significant inconsistency in their diameters and thickness was observed. In many cases, the filament got thicker or narrower, likely due to the solution's viscosity, surface tension, evaporations, and flow inconsistencies, among other influential production factors.

Figure 4.12 shows that the CFF filaments produced using solution 2 had a random orientation and did not follow any directional pattern. However, the filaments were extremely thin, with frequent occurrence of donut-shaped agglomerates. The fibers' thin web-like structure rendered the deposited CNF into a mat, making it hard to disperse in an asphalt binder. In addition, the observed agglomerates prevented the formation of strong filaments. The agglomerate formation is generally attributed to solution properties (Teo and Ramakrishna, 2006), solvent evaporation (Thompson et al., 2007), electrospinning parameters such as voltage, tip-to-collector distance, and flow rate (Huang et al., 2003), environmental conditions such as humidity and temperature (Casper et al., 2004) and polymer-solvent interactions due to compatibility issues (Li et al., 2004).

From Figure 4.13, it was found that the CNF filaments produced using solution 3, similar to those produced using solution 1, had a random orientation, did not follow any directional pattern, and were densely positioned to each other. However, inconsistencies in their diameters and thicknesses were observed. However, those inconsistencies were less frequent when compared with CNFs produced using solution 1.

From Figure 4.14, it was observed that the CNF filaments produced using solution 4 had a random orientation and were densely positioned with each other. In addition, frequent occurrence of drop-shaped agglomerates was evident. As noted earlier, the observed agglomerates prevented the formation of strong filaments. The fibers' dense matrix, proximity, and entanglements suggested a poor dispersion of the CNFs in the asphalt binder.

Figure 4.15 shows that the fiber structure of the CNFs produced using solution 5 is similar to that observed in nonwoven fabrics, as no distinct orientation in a specific direction in fiber alignment was observed. In addition, the CNF filament had a relatively consistent structure and smooth texture, with a rectangular cross-section with soft edges. Its smaller cross-sectional dimension is approximately two-thirds of its larger cross-sectional dimension. In addition, consistencies in the fibers' diameter, absence of a noticeable entanglement (compared with other CNFs), and low density and proximity of the produced filaments suggest an acceptable fiber dispersion in asphalt binder.

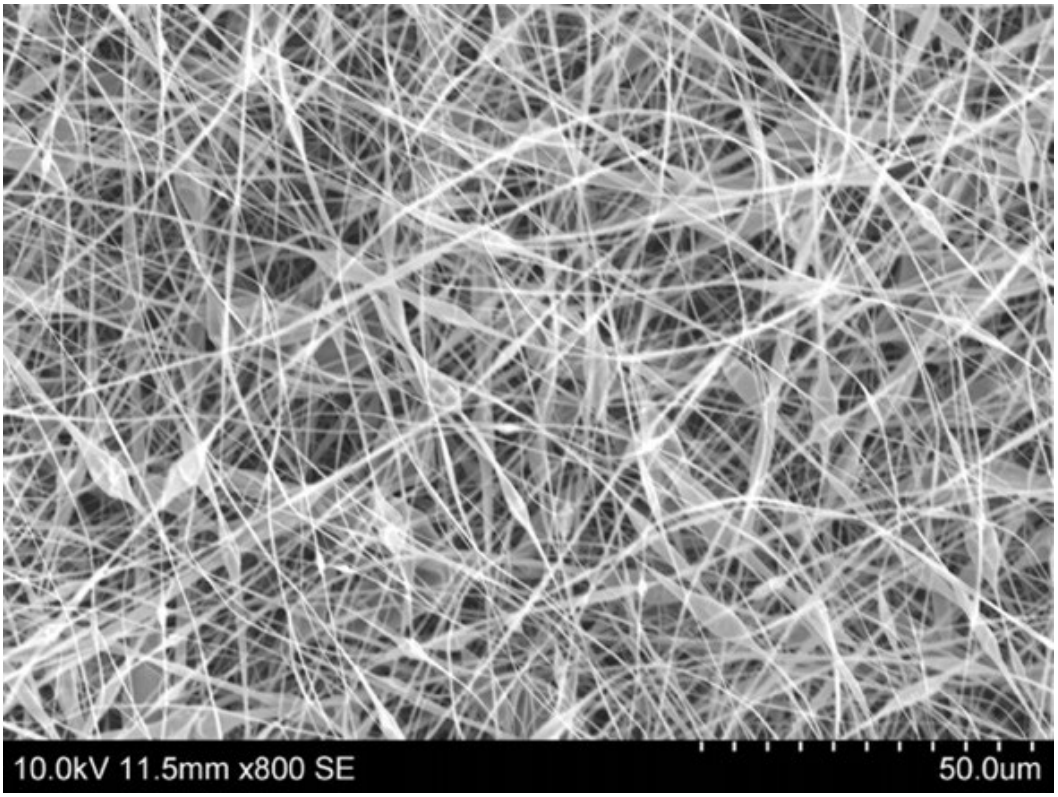

Figure 4.11 An SEM micrograph of the CNFs produced using solution 1

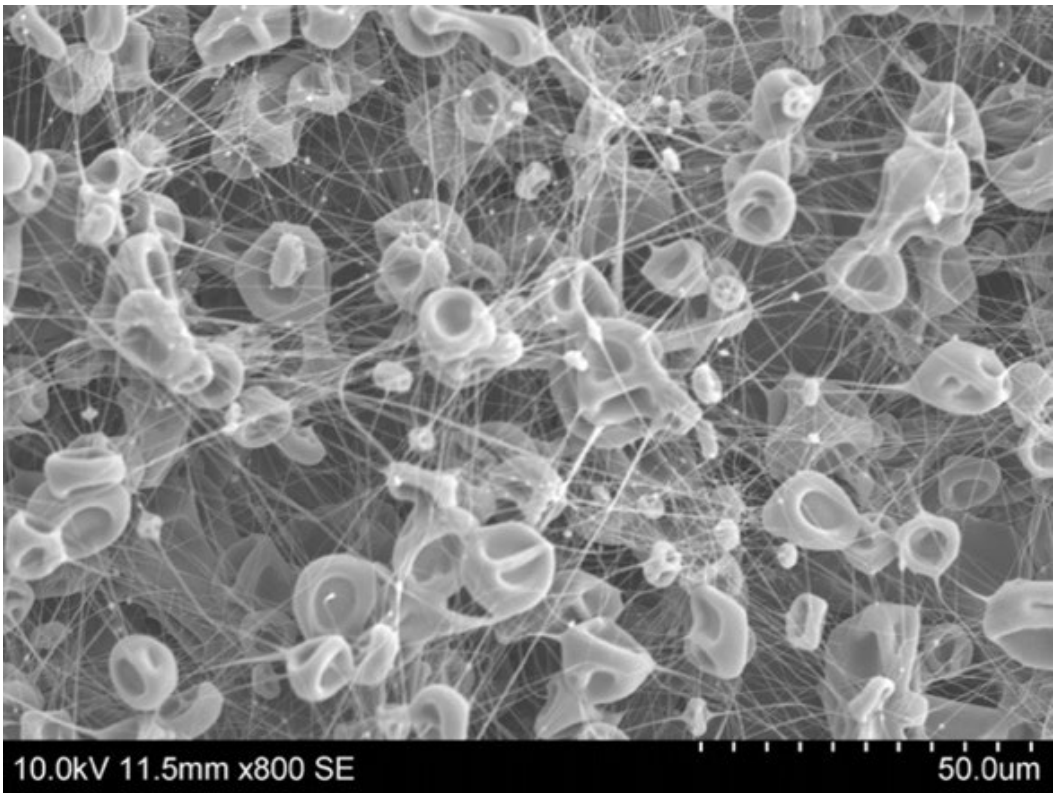

Figure 4.12 An SEM micrograph of the CNFs produced using solution 2

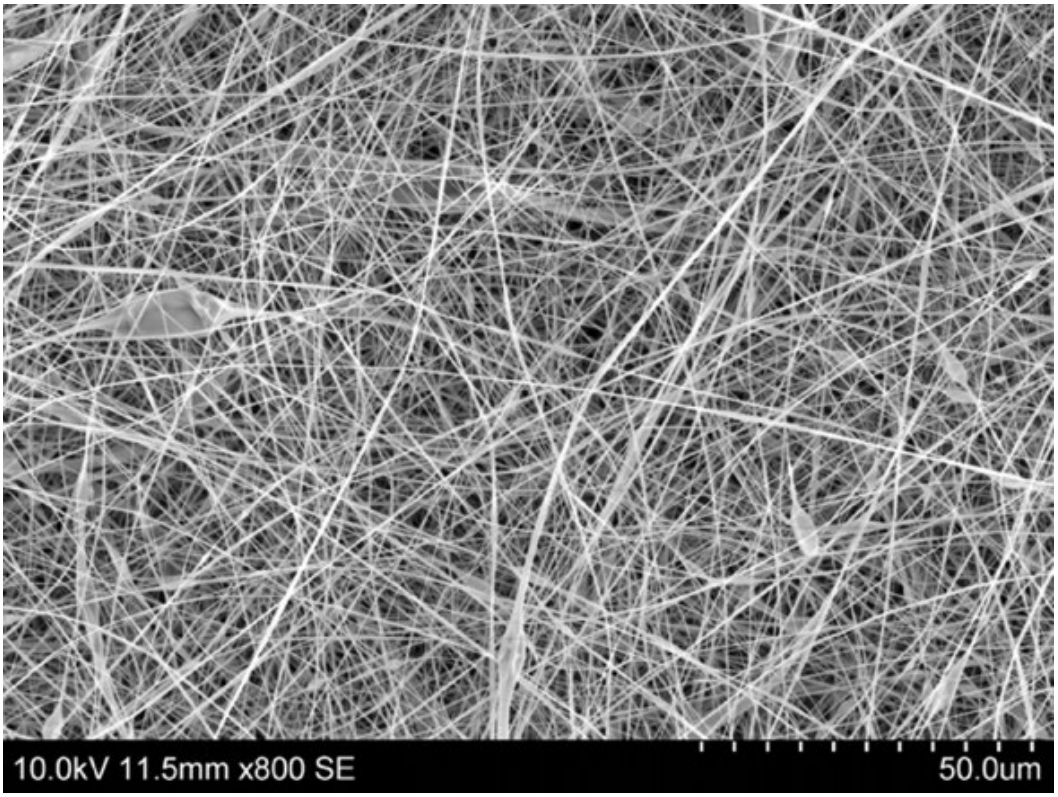

Figure 4.13 An SEM micrograph of the CNFs produced using solution 3

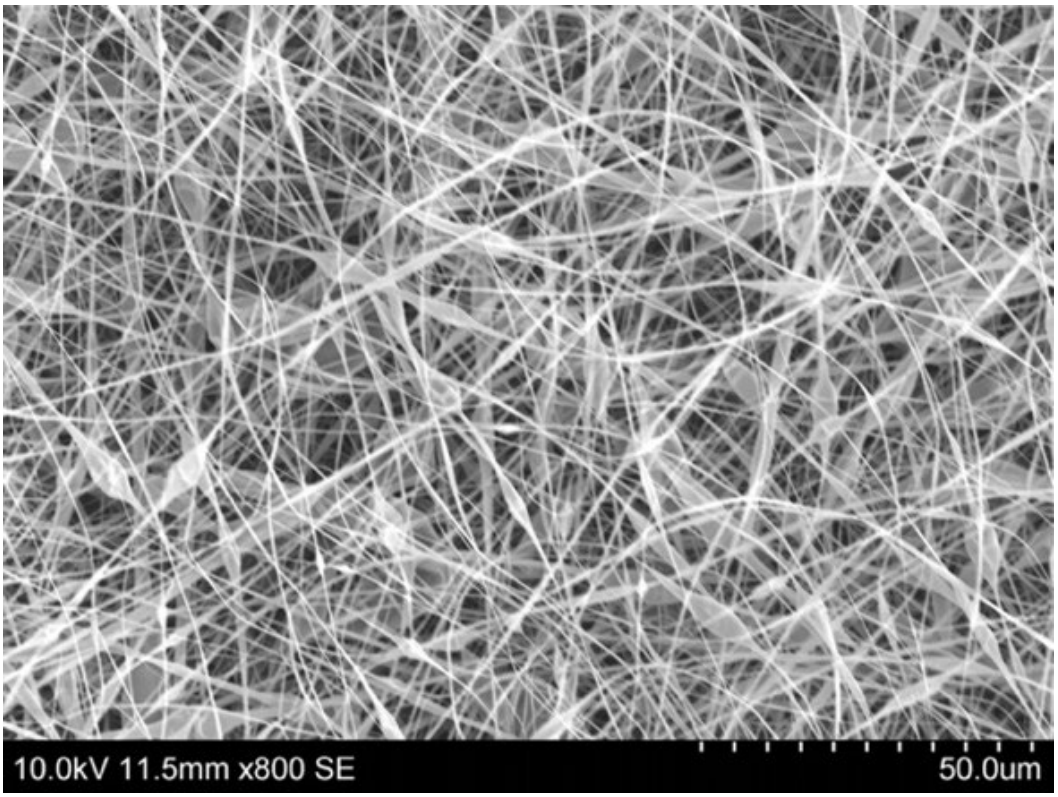

Figure 4.14 An SEM micrograph of the CNFs produced using solution 4

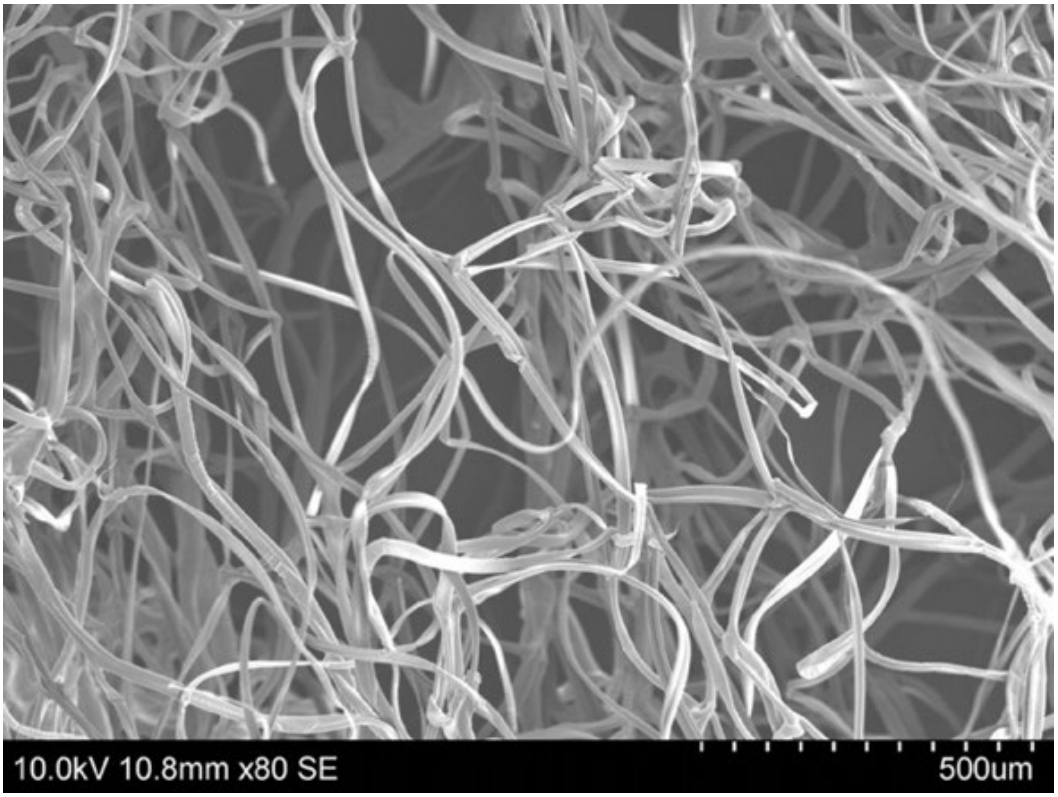

Figure 4.15 An SEM micrograph of the CNFs produced using solution 5

4.1.3 Tensile Strength of CNFs

The average tensile strength values of the CNF specimens produced using solutions 1, 2, 3, 4, and 5 and the rotating technique tested in production and cross-production directions are presented and summarized in Table 4.3.

Table 4.3 Tensile strength of CNFs produced using different solutions and rotating technique

Solution Type	Tested in Production Direction		Tested in Cross-Production Direction	
	Tensile Strength (specimens 1 and 2) (N)	Average Tensile Strength (N)	Tensile Strength (specimens 1 and 2) (N)	Average Tensile Strength (N)
Solution 1 (CA/Acetone)	7.9	7.8	9.3	8.3
	7.6		7.3	
Solution 2 (CA/Acetic Acid)	0.4	0.4	5.3	3.8
	0.3		2.2	
Solution 3 (CA/Acetic Acid/Water)	N/A	N/A	N/A	N/A
	N/A		N/A	
Solution 4 (CA/Acetic Acid/Acetone)	5	5.4	6.8	6.7
	5.7		6.6	
Solution 5 (CA/Acetone/Water)	2.3	2.5	2.5	1.9
	2.6		1.3	

Table 4.3 showed that the CNFs produced by rotating electrospinning of solution 1 produced fibers that had the highest average tensile strength values in the production direction (7.8 N) and cross-production direction (8.3 N) among other CNFs produced using different solutions and rotating techniques. The CNFs produced using solution 3 did not show a measurable tensile strength using the applied testing equipment.

The average tensile strength values of the CNF specimens produced using solutions 1, 2, 3, 4, and 5 and the static collector technique tested in two in-plane perpendicular directions (X and Y) are presented and summarized in Table 4.4.

Table 4.4 Tensile strength of CNFs produced using different solutions and static technique

Solution Type	Tested in X Direction		Tested in Y Direction	
	Tensile Strength (specimens 1 and 2) (N)	Average Tensile Strength (N)	Tensile Strength (specimens 1 and 2) (N)	Average Tensile Strength (N)
Solution 1 (CA/Acetone)	8.7	7.5	3.7	3.9
	6.2		4.0	
Solution 2 (CA/Acetic Acid)	N/A	N/A	N/A	N/A
	N/A		N/A	
Solution 3 (CA/Acetic Acid/Water)	N/A	N/A	N/A	N/A
	N/A		N/A	
Solution 4 (CA/Acetic Acid/Acetone)	3.9	4.2	3.4	3.9
	4.4		4.4	
Solution 5 (CA/Acetone/Water)	6.8	8.6	7.8	9.1
	10.4		10.3	

Table 4.4 shows that the CNFs produced by static collector electrospinning of solution 5 produced fibers with the highest average tensile strength values in the X direction (8.6 N) and Y direction (9.1 N), among other CNFs produced using different solutions. Table 4.4 also concludes that the average tensile strength of the CNF specimens tested in the X direction was 10% higher than that measured in the Y direction. Also, the average strain at failure for the specimens tested in the X direction was 3% less than that in the Y direction. In other words, the laboratory-produced electrospun CNF was stronger in the X direction and more ductile in the Y direction. It is important to note that the morphological and mechanical properties of the electrospun fibers are primarily influenced by the solvent type, its physical properties, and electrical conductivity Eda et al. (2007). Therefore, the strength and ductility of the fibers are expected to be adjustable as needed by altering the solvent's type and the CA's concentration. Also note that CNFs produced using solution 1 and the static collector method produced CNFs that also had tensile strengths higher than those produced using the rotating method. Given the findings from the visual inspections, SEM imaging results, and tensile strength values measured for the fibers, the CNFs produced with solution 5 and the static method are the optimal candidates for asphalt binder modification.

4.2 Results of the Tests Conducted on CNF-Modified Asphalt Binders

As described in the previous section, the CNFs produced with solution 5 and the static method are the optimal candidates for asphalt binder modification. For simplicity, from this point on, the selected CNF used for asphalt binder and mix modification will hereby be referred to as CNF.

4.2.1 Dynamic Viscosity

The effect of incorporating CNF in different asphalt binders on their dynamic viscosity was determined by conducting RV tests per the AASHTO T 316 (AASHTO, 2019) standard method. Figures 4.16, 4.17, and 4.18 summarize the dynamic viscosity values measured at 137°C and 167°C for PG 58-28, PG 64-34, and PG 70-28 asphalt binders without any CNF and those blended with 0.3 and 0.7% CNF by the binder weight, respectively. It is evident that the dynamic viscosity of all neat binders increased by an increase in the amount of incorporated CNF. For example, the dynamic viscosity of the PG 58-28 at 137°C (0.308 Pa.s) increased by 34% and 103% due to adding 0.3% and 0.7% CNF, respectively. A similar trend of variations in dynamic viscosity values of the PG 58-28 with different amounts of CNF was also observed when measured at 167°C. The dynamic viscosity of neat PG 58-28 tested at 167°C increased by 20% and 74% with the addition of 0.3% and 0.7% of CNF, respectively. The dynamic viscosity of the PG 64-34 at 137°C (0.867 Pa.s) increased by 13% and 36% due to adding 0.3% and 0.7% CNF to the blend, respectively. Furthermore, the dynamic viscosity of the PG 64-34 at 167°C (0.304 mPa.s) increased by 6% and 26% after blending it with 0.3% and 0.7% CNF. The dynamic viscosity of neat PG 70-28 at 137°C (1.175 Pa.s) increased by 23% and 46% due to adding 0.3% and 0.7% CNF to the blend, respectively. Finally, the dynamic viscosity values of the same binder measured at 167°C (0.404 Pa.s) increased by 65% and 107% due to blending it with 0.3% and 0.7% CNF, respectively. The preceding findings lead to concluding that an increase in CNF blended in asphalt binder increased the dynamic viscosity values of all tested binder blends. Overall, the effect of adding CNF to asphalt binders on increasing their viscosities was more pronounced at lower temperatures. While an increase in dynamic viscosity results in an increase in mixing and compaction temperatures, it is an indication of improved resistance to rutting (Hossain et al., 2014). Wu et al. (2007) also reported a change in visco-elastic properties of the asphalt mixes after incorporating fibers, which favors their resistance to rutting. In addition to the preceding observation, incorporating CNF in the polymer-modified asphalt binders (PG 64-34 and PG 70-28) resulted in different variation rates in the dynamic viscosity values compared with their non-polymer-modified counterparts. Xiao et al. (2014) reported that the viscosity of all asphalt binders is generally affected by polymer type, asphalt source, and test temperature. The high viscosity observed for the polymer-modified binders is due to the strong interaction between the polymer particles in the asphalt binder.

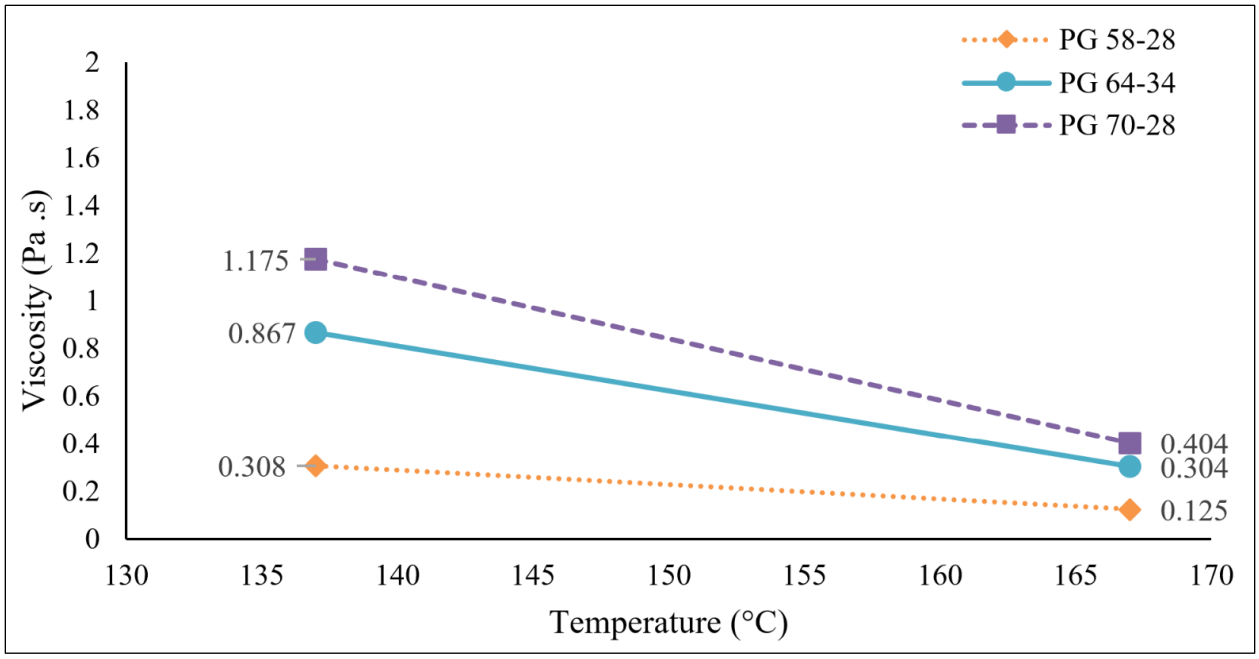

Figure 4.16 Dynamic viscosity values measured for PG 58-28, PG 64-34, and PG 70-28 asphalt binders measured at 137°C and 167°C

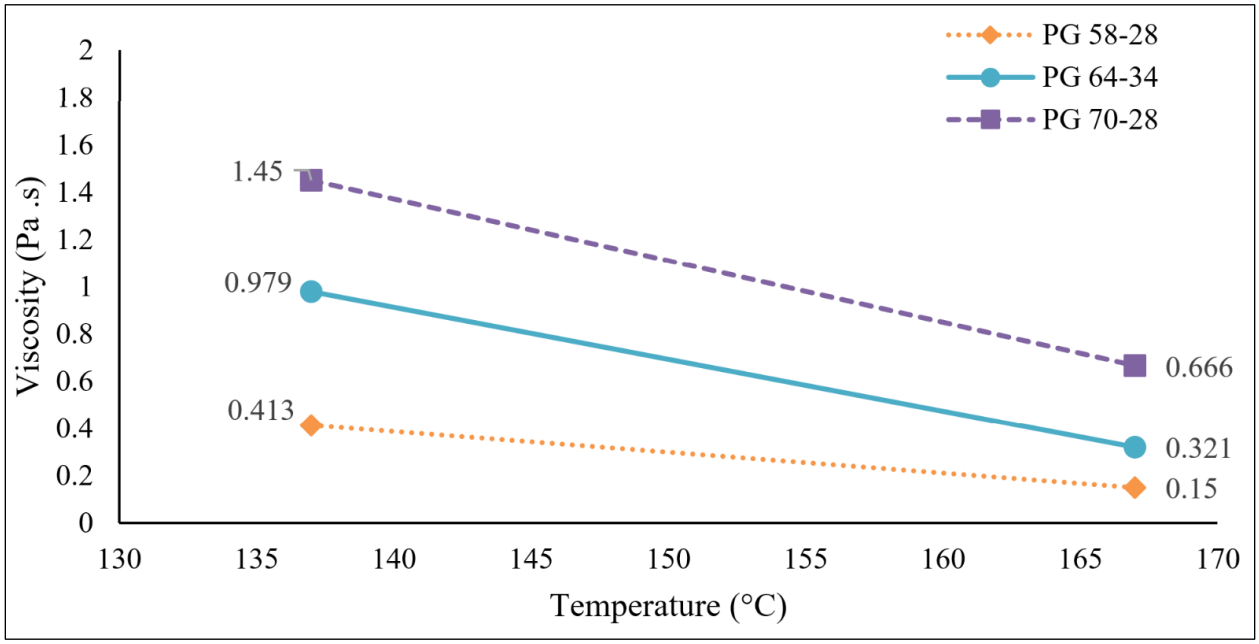

Figure 4.17 Dynamic viscosity values measured for PG 58-28, PG 64-34, and PG 70-28 binders containing 0.3% CNF measured at 137°C and 167°C

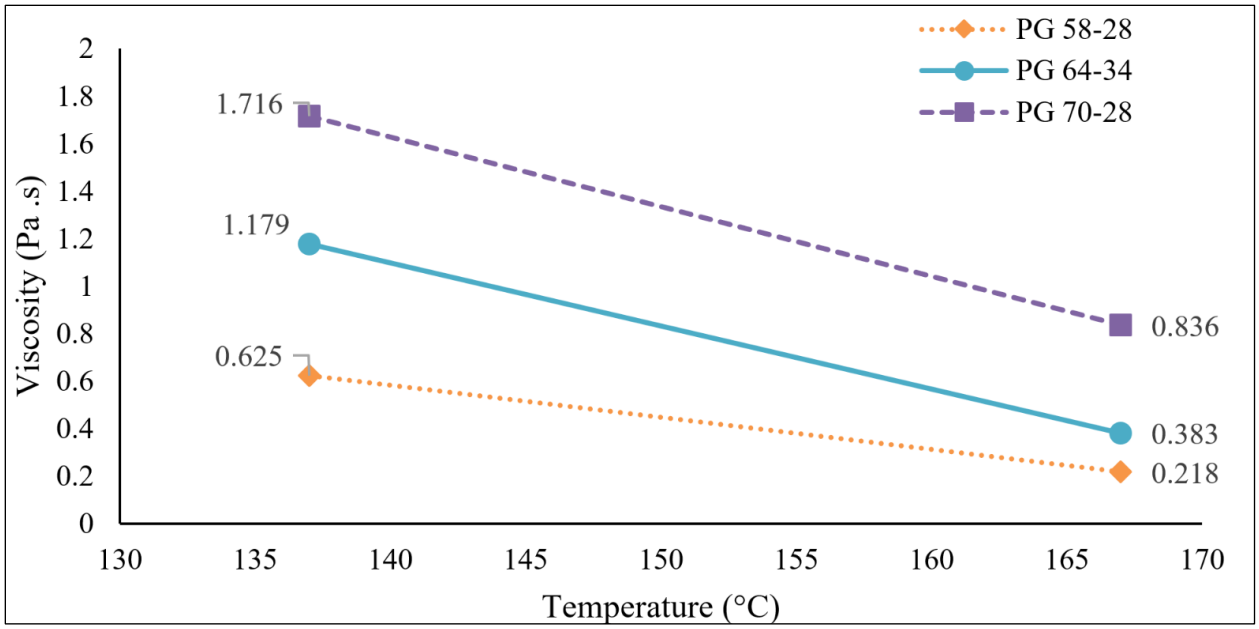

Figure 4.18 Dynamic viscosity values measured for PG 58-28, PG 64-34, and PG 70-28 binders containing 0.7% CNF measured at 137°C and 167°C

4.2.2 Fracture Energy

Figure 4.19 presents the absorbed fracture energy per unit cross-sectional area of the binder beam samples prepared with PG 58-28, PG 64-34, and PG 70-28 asphalt binder blends containing different amounts of CNF (0%, 0.2%, 0.3%, 0.5%, and 0.7%) tested at -14°C by an Izod pendulum machine following ASTM D256-10 (ASTM, 2018) standard method. Since applying this test for asphalt binder samples is a novel approach pursued in this study, CNF amounts were added at small increments to capture slight variations in absorbed energies due to changing CNF contents.

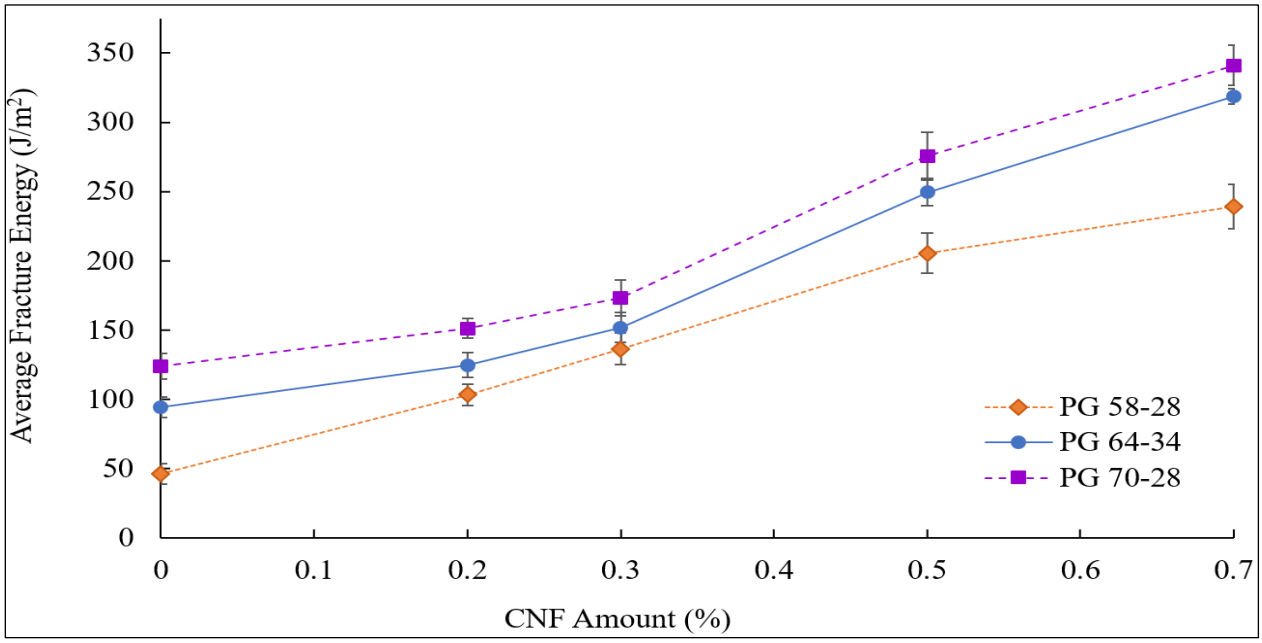

Figure 4.19 Fracture energy of asphalt binders blended with 0%, 0.2%, 0.3%, 0.5%, and 0.7% CNF

It is evident that the fracture energies increased with an increase in CNF content in all asphalt binder blends. For example, the absorbed fracture energy of the PG 58-28 asphalt binder increased by 124%, 195%, 345%, and 418% by incorporating 0.2%, 0.3%, 0.5%, and 0.7% CNF, respectively. Also, the absorbed fracture energy of the PG 64-34 binder increased by 32%, 61%, 165%, and 238% due to blending it with 0.2%, 0.3%, 0.5%, and 0.7% CNF, respectively. Finally, the absorbed fracture energy of the PG 70-28 asphalt binder increased by 22%, 40%, 122%, and 175% due to incorporating 0.2%, 0.3%, 0.5%, and 0.7% CNF, respectively. It can be concluded that the effect of adding CNF to asphalt binders on fracture energy was similar to that of incorporating polymers in binders. For example, neat PG 64-34 and PG 70-28 absorbed fracture energies were comparable to those measured for PG 58-28 containing 0.2% and 0.3% CNF. Therefore, incorporating CNF in asphalt binders is expected to favorably affect their resistance to cracking. Fracture energy-based methods are widely used to evaluate the resistance of asphalt mixes to cracking (e.g., Ozer et al., 2018; Al-Qadi et al., 2015; Mohammad et al., 2012; Ghabchi and Castro, 2021b). However, note that the application of Izod tests for evaluating asphalt binders was carried out with a limited scope only for this study. A comprehensive testing program is being pursued to establish a solid basis for validating and interpreting the Izod test results in the context of cracking potential in asphalt mixes.

4.2.3 Asphalt Binder-Aggregate Pull-off Strength

To study the effect of incorporating CNF in different binder blends on their adhesion to various types of aggregates while isolating the combined impact of the mix components, binder bond strength (BBS) tests were conducted on moisture-conditioned and dry specimens according to AASHTO T 361 standard method (AASHTO, 2016). This technique was applied to evaluate adhesion by measuring the pull-off strength and screening the aggregate-binder systems for the possibility of moisture-induced damage by conducting the tests on moisture-conditioned specimens.

4.2.3.1 Adhesion of Different Blends of Asphalt Binders Containing CNF to Granite

Table 4.5 summarizes the pull-off strength (POS) and pull-off strength ratio (PSR) values obtained by conducting BBS tests on dry and moisture-conditioned specimens of granite with PG 58-28, PG 64-34, and PG 70-28 asphalt binders without any CNF and those blended with 0.3% and 0.7% CNF and the extents of observed adhesive and cohesive failure mechanisms. The POS values of PG 64-34 and PG 70-28 binders measured for the granite specimens in dry condition (POS_{Dry}) increased with an increase in CNF content. For example, the POS_{Dry} value of the PG 64-34 with granite increased by 19% and 70%, respectively, due to incorporating 0.3% and 0.7% CNF in the binder. Similarly, the POS_{Dry} value of PG 70-28 with granite after adding 0.3% and 0.7% CNF to the blend increased by 0.1% and 10%, respectively. An improvement in adhesion between asphalt binder and aggregate is reported to increase the mix's resistance to fatigue cracking (Júnior et al., 2020), improve resistance to raveling (Mo et al., 2010), and significantly contribute to overall durability of an asphalt mix (Moraes et al., 2011). The variations in the POS_{Dry} value of the granite samples prepared with PG 58-28 binder decreased by 23% and 10%, respectively, after using 0.3% and 0.7% CNF in the blend. Note that the effectiveness of any additive such as CNF in an asphalt binder is governed by the mechanical properties of each phase (asphalt, additive, and aggregate), and it also depends on their physiochemical compatibilities to form a strong bond. The observed reduction in pull-off strength developed between granite and PG 58-28 asphalt binder after the addition of CNF can be due to the physiochemical incompatibility of the phases present in the aggregate-binder-CNF system.

Table 4.5 POS and PSR values and binder-aggregate failure mechanisms measured for binder blends containing 0%, 0.3%, and 0.7% CNF with granite

Asphalt Binder Type	CNF Amount	Dry				Moisture-Conditioned				PSR Value (POS_{Wet}/POS_{Dry})
		POS (kPa)	SD (%)	COV (%)	Failure Type	POS (kPa)	SD (%)	COV (%)	Failure Type	
PG 58-28	0% CNF	139.1	9.2	6.6	99% Cohesive	107.0	13.2	12.3	96% Cohesive	0.77
	0.3% CNF	106.5	4.1	3.8	98% Cohesive	106.9	2.5	2.4	79% Cohesive	1.00
	0.7% CNF	124.7	4.7	3.8	92% Cohesive	114.8	3.4	3.0	88% Cohesive	0.92
PG 64-34	0% CNF	62.9	6.4	10.2	97% Cohesive	54.4	2.7	4.9	85% Cohesive	0.87
	0.3% CNF	74.7	7.8	10.4	96% Cohesive	56.9	1.8	3.2	79% Cohesive	0.76
	0.7% CNF	106.7	7.3	6.9	99% Cohesive	88.9	9.4	10.6	70% Cohesive	0.83
PG 70-28	0% CNF	126.4	6.9	5.5	94% Cohesive	92.2	16.1	17.4	79% Adhesive	0.73
	0.3% CNF	126.5	8.6	6.8	98% Cohesive	76.2	18.3	24.1	78% Adhesive	0.60
	0.7% CNF	139.2	57.6	41.4	97% Cohesive	112.5	6.5	5.8	70% Adhesive	0.81

Table 4.5 shows that the PSR value of the PG 58-28 with granite (0.77) became 1.00 and 0.92 due to adding 0.3% and 0.7% CNF to the binder, respectively. Also, the failure mechanism of the samples mainly remained cohesive before and after moisture conditioning. In other words, blending PG 58-28 binder with CNF when used with granite aggregate is expected to improve the mix's resistance to moisture-induced damage. Furthermore, the PSR value of the granite samples prepared with PG 64-34 binder (0.86) became 0.76 and 0.83, respectively, after using 0.3% and 0.7% CNF in binder blends. While this indicates a slight reduction in PSR values as a result of using CNF in the binder, conducting a two-tailed test (significance level α=0.05) suggests that the differences between the POS_{Dry} and POS_{Wet} values observed for each blend of PG 58-28 with CNF (0, 0.3, and 0.7) and granite were not statistically significant. Therefore, the moisture-induced damage potential of asphalt mixes containing PG 64-34 binder and granite was not significantly affected by using CNF in the mix. Moreover, the PSR value of the PG 70-28 binder with granite (0.73) after incorporating 0.3% and 0.7% CNF changed to 0.60 and 0.81, respectively. While this is a mixed variation trend, the extent of cohesive failure became more prominent with an increase in CNF amount. For example, the 21% cohesive failure mechanism for PG 70-28 with granite increased to 22% and 30% cohesive failure after using 0.3% and 0.7% CNF in the blend, respectively. These observations may conclude that adding a high amount of CNF (0.7%) to PG 70-28 binder when used in a mix with mainly granite aggregate may slightly improve its resistance to moisture-induced damage.

4.2.3.2 Adhesion of Different Blends of Asphalt Binders Containing CNF to Quartzite

The POS_{Dry}, POS_{Wet}, and PSR values were measured for dry and moisture-conditioned BBS specimens of quartzite prepared with PG 58-28, PG 64-34, and PG 70-28 asphalt binders without any CNF and those containing 0.3 and 0.7% CNF (summarized in Table 4.6). Also, the extents of their observed failure mechanisms are outlined. Note these examples: The POS_{Dry} value of the PG 64-34 with quartzite consistently increased with an increase in CNF content. The POS_{Dry} value of the PG 64-34 with quartzite increased by 10% and 75%, respectively, due to using 0.3% and 0.7% CNF in the binder blends. The PG 70-28 binder showed a slight reduction (8%) and an increase (9%) in POSDry values after adding 0.3% and 0.7% CNF to the blend, respectively. As discussed earlier, an improved adhesion is expected to result in mixes with improved durability and boosted performance against rutting, cracking, and raveling (Júnior

et al., 2020; Mo et al., 2010; Moraes et al., 2011). The POS_{Dry} value of the quartzite samples prepared with PG 58-28 decreased by 13% and 26%, respectively, after the incorporation of 0.3% and 0.7% CNF in the blend. A similar trend of variation in POS_{Dry} for PG 58-28 binder with quartzite was also observed with granite and associated with the physiochemical incompatibility of phases in the aggregate-binder-CNF system.

Table 4.6 POS and PSR values and binder-aggregate failure mechanisms measured for binder blends containing 0%, 0.3%, and 0.7% CNF with quartzite

Asphalt Binder Type	CNF Amount	Dry				Moisture-Conditioned				PSR Value (POS_{Wet}/POS_{Dry})
		POS (kPa)	SD (%)	COV (%)	Failure Type	POS (kPa)	SD (%)	COV (%)	Failure Type	
PG 58-28	0% CNF	133.7	12.3	9.2	98% Cohesive	177.3	4.6	2.6	89% Cohesive	1.33
	0.3% CNF	115.9	7.9	6.8	98% Cohesive	144.0	2.3	1.6	88% Cohesive	1.24
	0.7% CNF	99.5	18.3	18.4	98% Cohesive	160.6	3.6	2.2	62% Cohesive	1.62
PG 64-34	0% CNF	60.0	7.5	12.5	96% Cohesive	56.2	5.5	9.7	96% Cohesive	0.94
	0.3% CNF	66.1	2.9	4.4	96% Cohesive	83.8	31.8	38.0	94% Cohesive	1.27
	0.7% CNF	105.0	43.1	41.0	97% Cohesive	133.5	50.7	38.0	94% Cohesive	1.27
PG 70-28	0% CNF	114.0	7.4	6.5	91% Cohesive	148.4	56.4	38.0	54% Cohesive	1.30
	0.3% CNF	104.6	3.5	3.4	95% Cohesive	121.0	10.8	8.9	92% Cohesive	1.16
	0.7% CNF	124.2	6.6	5.3	98% Cohesive	172.3	65.9	38.2	95% Cohesive	1.39

Table 4.6 shows that the PSR value of the PG 58-28 binder with quartzite (1.33) became 1.24 and 1.61, respectively, as a result of the addition of 0.3% and 0.7% CNF to the binder, an indication of strong resistance to moisture-induced damage before and after using CNF in the blend. While the failure mechanism remained cohesive primarily before and after moisture conditioning, the adhesive failure mechanism increased from 2% to 36% due to incorporating 0.7% CNF in the binder blend. Similarly, from Figure 16, the PSR value of the granite samples prepared with PG 64-34 binder (0.94) increased to 1.27 after adding 0.3% and 0.7% CNF to asphalt binder blends. In other words, adding CNF to PG 64-34 asphalt binder is expected to improve the asphalt mix's resistance to moisture-induced damage. The fracture mechanisms also remained mostly cohesive, even after moisture conditioning, indicating a high resistance to moisture-induced damage. Finally, the PSR value of the PG 70-28 binder with quartzite (1.30) after incorporating 0.3% and 0.7% CNF remained greater than 1 and changed to 1.16 and 1.39, respectively, indicating high resistance to moisture-induced damage. Additionally, the failure mechanism of quartzite samples after moisture-conditioning, 52% cohesive for PG 70-28 binder, shifted to 92% and 95% cohesive, which supports the notion of improvement in the mix's resistance to moisture-induced damage as a result of using CNF in the binder. Overall, it can be concluded that asphalt mixes prepared with quartzite aggregates and any of the studied asphalt binders (PG 58-28, PG 64-34, and PG 70-28) containing CNF are expected to exhibit a high resistance to moisture-induced damage.

4.2.3.3 Adhesion of Different Blends of Asphalt Binders Containing CNF to Gravel

Table 4.7 summarizes the POS and PSR values measured for dry and moisture-conditioned gravel BBS specimens prepared with PG 58-28, PG 64-34, and PG 70-28 asphalt binders without any CNF and those containing 0.3 and 0.7% CNF. The extents of their observed failure mechanisms are also outlined. For instance, the POS_{Dry} values of gravel BBS specimens prepared with both PG 64-34 and PG 70-28 binders increased with an increase in their CNF contents. Additionally, gravel BBS specimens prepared with PG 64-34 asphalt binder exhibited POS_{Dry} values of 15% and 96% higher than neat binder after adding 0.3% and 0.7% CNF, respectively. Similarly, the POS_{Dry} value of gravel BBS specimens prepared with PG 64-34 binder after incorporating 0.3% and 0.7% CNF in the blend increased by 2% and 17%, respectively. Therefore, one can conclude that asphalt mixes containing PG 64-34 or PG 70-28 asphalt binders and gravel aggregates are expected to exhibit improved durability and overall performance as a result of strong asphalt binder-aggregate adhesion (Moraes et al., 2011). However, gravel BBS samples prepared with PG 58-28 binder experienced 38% and 40% reduction in their POS_{Dry} values compared with the neat binder due to blending it with 0.3% and 0.7% CNF, respectively. Similar observations were also made for granite and quartzite BBS samples prepared with different blends of CNF and PG 58-28 binder. As noted earlier, the observed reduction in POS_{Dry} values due to incorporating CNF in PG 58-28 binder with different aggregates was attributed to incompatibilities of the various material phases participating in adhesion.

Table 4.7 POS and PSR values and binder-aggregate failure mechanisms measured for binder blends containing 0%, 0.3%, and 0.7% CNF with gravel

Asphalt Binder Type	CNF Amount	Dry				Moisture-Conditioned				PSR Value (POS_{Wet}/POS_{Dry})
		POS (kPa)	SD (%)	COV (%)	Failure Type	POS (kPa)	SD (%)	COV (%)	Failure Type	
PG 58-28	0% CNF	150.9	9.2	6.1	94% Cohesive	176.0	6.0	3.4	78% Cohesive	1.17
	0.3% CNF	93.4	15.7	16.8	95% Cohesive	108.9	5.9	5.4	85% Cohesive	1.17
	0.7% CNF	90.2	11.2	12.4	84% Cohesive	148.0	4.2	2.8	82% Cohesive	1.64
PG 64-34	0% CNF	59.5	3.1	5.3	94% Cohesive	57.2	4.0	7.0	89% Cohesive	0.96
	0.3% CNF	68.3	5.8	8.5	91% Cohesive	80.8	30.7	38.0	96% Cohesive	1.18
	0.7% CNF	116.4	6.7	5.8	99% Cohesive	134.2	6.1	4.5	97% Cohesive	1.15
PG 70-28	0% CNF	107.2	3.6	3.3	79% Cohesive	133.4	5.8	4.3	74% Cohesive	1.24
	0.3% CNF	109.8	7.7	7.0	93% Cohesive	143.3	13.8	9.6	86% Cohesive	1.31
	0.7% CNF	125.0	2.2	1.7	96% Cohesive	136.9	5.4	3.9	93% Cohesive	1.10

Note that asphalt binders, based on their crude oil source, differ in their chemical compositions. Also, different types of chemicals may be added to asphalt binders in the refineries (e.g., polyphosphoric acid) to improve their mechanical properties. Those chemicals (existing in crude oil or added in the refinery) may interact with other additives used in the binder and adversely affect the mechanical properties of the binder blends. Since incorporating CNF in PG 58-28 was found to reduce the blends' adhesion with all three aggregates consistently, this hypothesis is more likely to be valid. Nevertheless, elemental analysis of asphalt binder is recommended to further research the effect of the binder's chemical composition on its adhesion with different aggregates in the presence of CNF.

Additionally, the PSR value of PG 58-28 with gravel (1.17) remained at 1.17 and increased to 1.64 due to incorporating 0.3% and 0.7% CNF in the binder, respectively. Similarly, the PSR value of the gravel BBS samples prepared with PG 64-34 binder (0.96) increased to 1.18 and 1.15, respectively, due to using 0.3% and 0.7% CNF in binder blends. The observed increase in PSR values with an increase in CNF content suggests that incorporating CNF in PG 58-28 or PG 70-28 binder when used with gravel aggregate is expected to benefit the resistance of the mix to moisture-induced damage. Also, despite a slight increase in adhesive failure mode, the failure mechanism of the gravel BBS samples of both PG 58-28 and PG 64-34 binders containing CNF remained mostly cohesive after moisture conditioning. The remaining failure surface within the asphalt binder-CNF matrix (cohesive failure) after moisture conditioning suggests insignificant decay in adhesion of the binder with aggregate, confirming the favorable effect of CNF on the mixes' resistance to moisture-induced damage. Finally, the average PSR value measured for gravel BBS specimens prepared with PG 70-28 binder (1.24) remained greater than 1 after mixing it with 0.3% and 0.7% CNF and became 1.31 and 1.10, respectively. In addition, the failure mechanism of gravel BBS samples prepared with PG 70-28 binder containing different amounts of CNF after moisture conditioning remained mostly cohesive, similar to their dry-conditioned counterparts. These observations lead to the conclusion that the asphalt mixes prepared with mainly gravel and PG 70-28 binder blended with different CNF amounts are expected to have an acceptable resistance to moisture-induced damage.

4.3 Results of the Tests Conducted on Asphalt Mixes

4.3.1 Resistance to Cracking

The SCB tests following the ASTM D8044-16 (ASTM, 2016) standard method were conducted on HMA mixes containing 0%, 0.3%, and 0.7% CNF by the weight of asphalt binder to evaluate the effect of incorporating CNF in asphalt mixes on their resistance to cracking. Details of the asphalt mixes were discussed earlier and presented in Table 3.4 and Figure 3.5. The critical strain energy release rate (J_c) values obtained by conducting SCB tests on the HMA mix without any CNF and those containing 0.3% and 0.7% CNF by the weight of the binder are presented in Figure 4.20. The J_c values measured for the HMA mix significantly increased with increased incorporation of CNF. For example, the J_c values of the HMA mixes containing 0%, 0.3%, and 0.7% by the weight of asphalt binder were found to be 0.53, 0.72, and 0.98, respectively. In other words, the J_c value of the HMA containing no CNF increased by 19% and 45%, respectively, as a result of using 0.3% and 0.7% CNF by the weight of asphalt binder in the mix. As the J_c value increases, an asphalt mix's resistance to cracking increases (Mohammad et al., 2012; 2004). A J_c value greater than 0.5 is recommended by the ASTM D8044-16 (ASTM, 2016) for a mix with an acceptable resistance to cracking. Based on these observations, incorporating CNF in an asphalt mix is expected to significantly improve its resistance to cracking. This finding agrees with the increase in average fracture energy due to incorporating CNF in different asphalt binders observed in the Izod impact resistance test, as discussed in section 4.2.2.

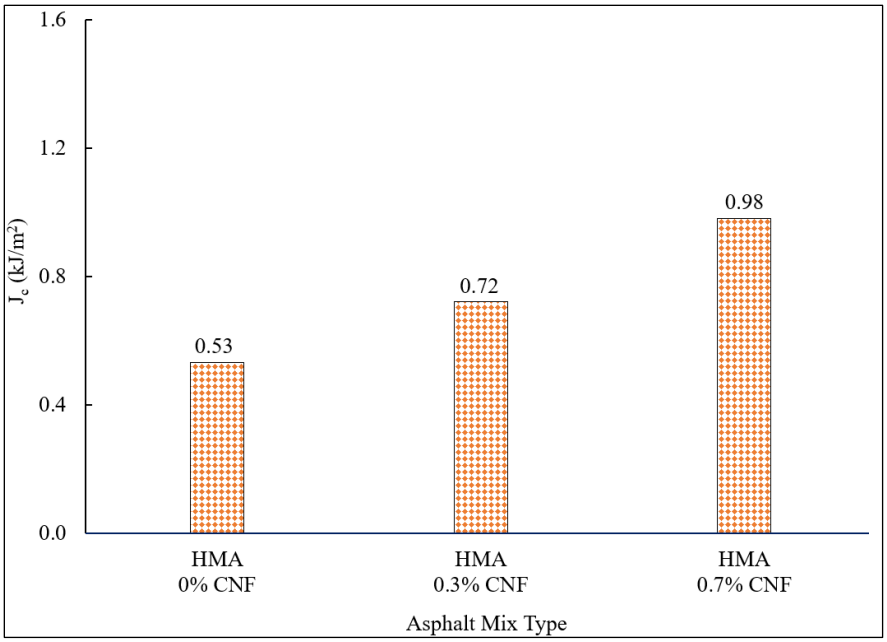

Figure 4.20 Critical strain energy release rate (J_c) of the tested mixes

4.3.2 Resistance to Rutting and Stripping

A Hamburg wheel tracking (HWT) test following the AASHTO T 324 standard test method (AASHTO, 2019) was conducted to evaluate the effect of incorporating CNF in asphalt mixes on their resistance to rutting and moisture-induced damage. Figure 4.21 presents the rut depths measured at different numbers of wheel passes obtained from conducting the HWT tests. Rut depths shown in Figure 4.21 are average deformation measurements from the right and left wheels for the tests conducted on a double-wheel HWT machine. Tests on the HMA sample containing 0.3% CNF were repeated due to an error in water temperature. The rut depths measured for the HMA mix without CNF were found to be 4.4, 6.2, and 11.5 mm at 5,000, 10,000, and 15,000 wheel passes. A stripping inflection point (SIP) was also detected at 11,355 wheel passes, suggesting the onset of moisture-induced damage.

Additionally, the rut depths measured for the HMA mix containing 0.3% CNF by the weight of binder were 3.9, 5.3, and 10.3 mm at 5,000, 10,000, and 15,000 wheel passes, with a SIP occurring at 12,610 wheel passes. In other words, the measured rut depths for the mix containing 0.3% CNF were, on average, 12% less than those without CNF. Moreover, the wheel passes corresponding to a SIP observed in the mix containing 0.3% CNF was 11% higher than that measured for the mix containing 0.3% CNF, suggesting an improved resistance to moisture-induced damage due to adding CNF to the mix. Similarly, the mix containing 0.7% CNF by the weight of the binder exhibited rut depths of 3.6, 5.0, and 9.9 mm at 5,000, 10,000, and 15,000 wheel passes, with a SIP at 12,590 wheel passes. In short, the rut depths measured for the mix containing 0.7% CNF were, on average, 11% less than those recorded without CNF. The favorable effect of incorporating fibers in asphalt mixes on their resistance to rutting was also reported by Wu et al. (2007) by conducting dynamic modulus tests on mixes containing different types of fibers. Asphalt mixes improved their elastic properties at high temperatures after adding fibers, indicative of an improved resistance to rutting. Additionally, the SIP measured for the mix containing 0.7% CNF was observed at wheel passes 11% higher than those measured for the mix without any CNF. Therefore, it is concluded that the use of 0.3% and 0.7% CNF is expected to increase the mix's resistance to both rutting and moisture-induced damage.

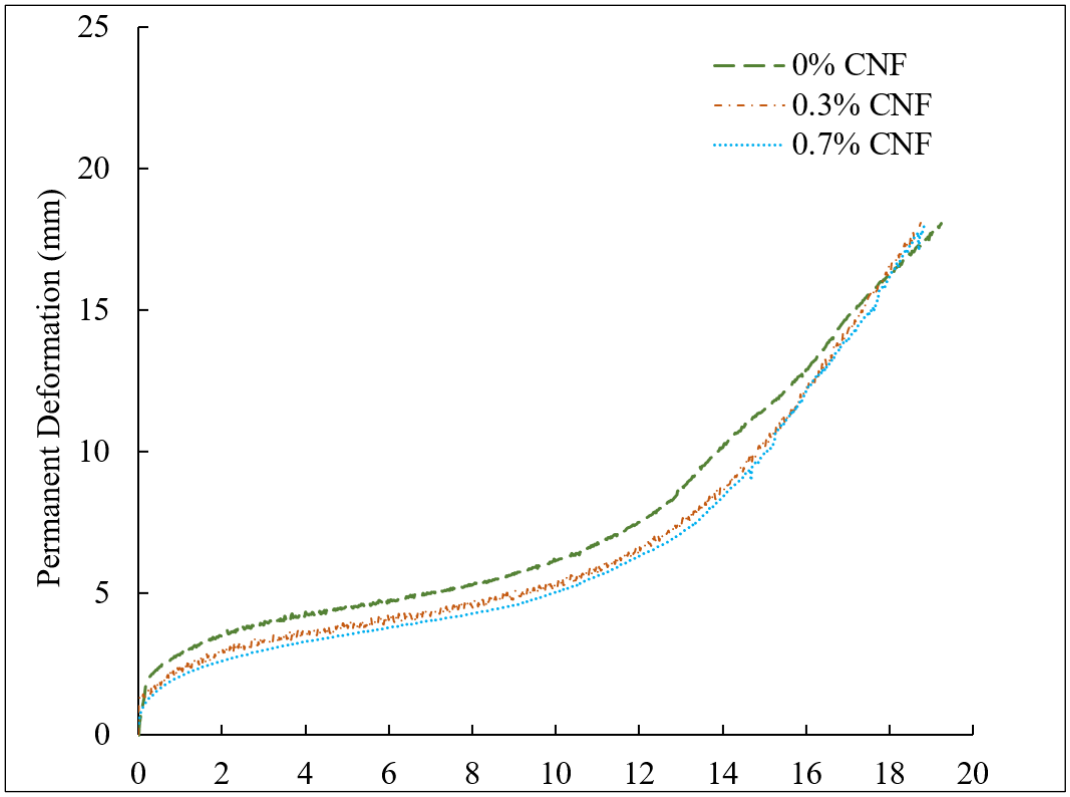

Figure 4.21 Measured permanent deformations with wheel passes for asphalt mixes

4.3.3 Resistance to Moisture-Induced Damage

Figure 4.22 shows the average indirect tensile strength (ITS) values measured for dry (ITS_{Dry}) and moisture-conditioned (ITS_{Wet}) specimens and their corresponding TSR values obtained from testing asphalt mixes following the AASHTO T 283 (AASHTO, 2014) standard method. Only the asphalt mix without any CNF (HMA 0% CNF) met the minimum TSR requirement (≥ 0.8) set by AASHTO T 283 (AASHTO, 2014). The TSR values measured for the HMA mixes containing 0%, 0.3%, and 0.7% CNF by the weight of the binder were found to be 0.86, 0.66, and 0.72. From these findings, the asphalt mix under study appears to partially lose resistance to moisture-induced damage by adding 0.3% CNF and gain some back by incorporating 0.7% CNF in the mix. However, the ITS_{Dry} value of the HMA containing 0% CNF increased by 9% and 24% as a result of using 0.3% and 0.7% CNF in the mix. This contributes to the observed reduction in TSR values with an increase in CNF amount. For example, ITS_{Dry} and ITS_{wet} values measured for the mix containing 0.7% CNF were 24% and 4%, respectively, higher than those without CNF. However, the TSR value measured for the mix containing 0.7% CNF was 16% less than that of the mix containing no CNF. In contrast, the HWT test results, as discussed in section 4.3.2, indicated that adding CNF by 0.3% and 0.7% to the asphalt mix improved its resistance to moisture-induced damage. While both HWT and TSR tests are empirical, the HWT test, due to its cyclic wheel loading, is believed to better simulate in-service conditions of an asphalt pavement than the TSR test (Lu and Harvey, 2006). The BBS test findings, in general, suggest an improvement in the binder-aggregate systems' resistance to moisture-induced damage due to incorporating CNF in studied asphalt binders. Similar TSR shortcomings have been discussed by several studies (e.g., Ghabchi et al., 2016, 2014; Ghabchi and Castro, 2021a; Hanz, 2007; Birgisson et al., 2005). The TSR test was originally developed for conventional asphalt mixes, and its current form may not be the most realistic method for evaluating moisture-induced damage in new materials such as those discussed herein.

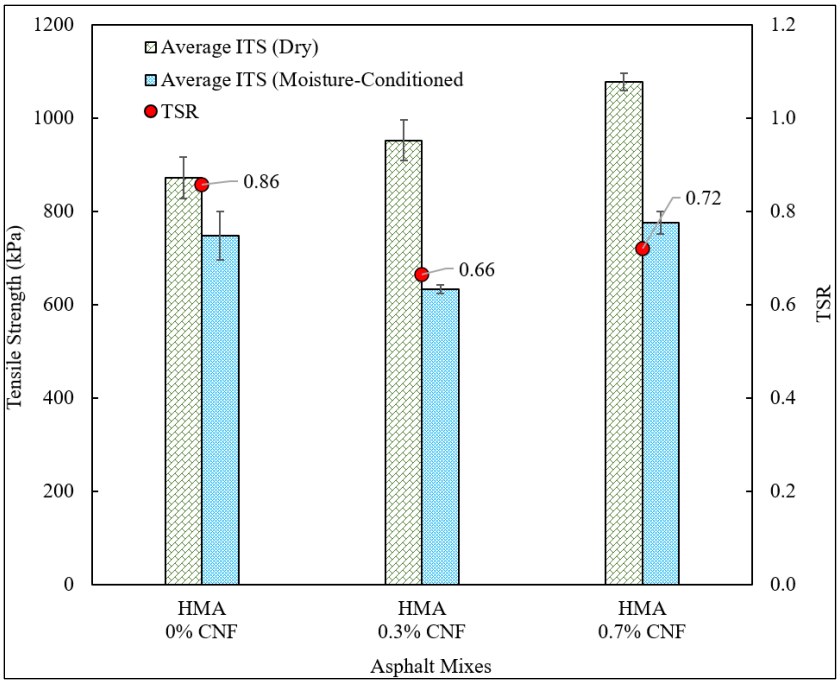

Figure 4.22 ITS and TSR values measured for dry and moisture-conditioned samples

5. CONCLUSIONS AND RECOMMENDATIONS

The feasibility of producing cellulose nanofibers (CNF) in the laboratory using the electrospinning method was evaluated. The produced CNF was characterized by conducting scanning electron microscopy (SEM) imaging and tensile strength tests. The effects of using different CNF amounts in various types of asphalt binders—PG 58-28, PG 64-34, and PG 70-28—on binder blends' dynamic viscosity, resistance to cracking, and adhesion to different aggregates were evaluated by conducting rotational viscometer (RV), Izod impact, and binder bond strength (BBS) tests, respectively. The effects of incorporating 0%, 0.3%, and 0.7% CNF on cracking, rutting, and moisture-induced damage potential of asphalt mixes were characterized by conducting semi-circular bend (SCB), Hamburg wheel tracking (HWT), and tensile strength ratio (TSR) tests, respectively. Based on the results, discussions, and observations in this study, conclusions were drawn as follows.

1. Electrospinning was a flexible, quick, scalable, and inexpensive method for producing CNF with consistent quality as an asphalt additive. The structure and morphology of the produced CNF were randomly oriented, similar to nonwoven fabrics with a soft-edged rectangular filament cross-section.

2. The produced CNF was found to have tensile strength values that, on average, differed by 10% when tested in two perpendicular directions. The strain at failure measured in the direction with a higher tensile strength was, on average, 3% less than that measured in the other direction.

3. Incorporating CNF in asphalt binders was found to increase the dynamic viscosity values of all tested binder blends. The effect of adding CNF to asphalt binders on increasing their viscosities was more pronounced at lower temperatures for all binders (PG 58-28, PG 64-34, and PG 70-28) and more prominent in the non-polymer-modified binder (PG 58-28). An increase in dynamic viscosity increased mixing and compaction temperatures. It is also expected to be indicative of an improved resistance to rutting.

4. Absorbed fracture energy determined by conducting the Izod pendulum impact test was introduced as an innovative adoption of an existing test method for quick characterization of asphalt binders' resistance to cracking. A beam sample preparation procedure was developed and discussed. An increase in the amount of CNF added to binders resulted in a consistent rise in average absorbed fracture energy values measured for all types of asphalt binders. It was found that the effect of adding CNF to asphalt binders on absorbed fracture energy values was similar to that observed due to using polymer-modified binders.

5. The results of BBS tests indicated an overall improvement in the adhesion of asphalt binders to tested aggregates due to CNF incorporation in binder blends.

6. Asphalt mixes' resistance to cracking, determined by conducting SCB tests, was significantly improved due to incorporating CNF in the mixes.

7. Based on the HWT test results, using CNF in asphalt mixes effectively reduced the mixes' susceptibility to rutting and moisture-induced damage.

8. The results of TSR tests conducted on asphalt mixes did not completely agree with HWT test results. While it showed an improvement in tensile strength values of the dry and moisture-conditioned samples due to using 0.7% CNF compared with that containing 0% CNF, the one without CNF still exhibited a higher TSR value. This finding was attributed to the empirical nature of the TSR test, which underlines the importance of using tests with a more robust mechanistic basis to screen new generations of asphalt mixes for moisture-induced damage.

It is recommended to use other electrospinning technique variations to explore the effects of different solvents, different concentrations of cellulose acetate, temperature, voltage, and tip-to-collector distance on the produced CNF's mechanical properties. An elemental analysis on asphalt binders is also recommended to investigate any chemical incompatibilities of the CNF with the asphalt binder's chemical composition, which may result in a weak bond with aggregates. Given the methodology used in this study, every batch of CNF-modified asphalt binder was shear-mixed as needed and used for sample preparation immediately after the shear-mixing procedure was complete. This process alleviated concerns related to homogeneity and uniformity of CNF dispersion in the binder due to omitting any time gaps between mixing and using the binder blends for sample preparation. This simulates asphalt plant CNF-binder blending. With terminal blending, the storage stability of a CNF-modified asphalt binder is recommended for future study. In this study, applying the Izod impact test for evaluating asphalt binders was carried out with a limited scope. A separate study is recommended to establish a solid basis for validating and interpreting the Izod test results in characterizing cracking potential in asphalt mixes.

6. REFERENCES

[1] AASHTO M 323, 2017. "Standard Specification for Superpave Volumetric Mix Design." *Standard Specifications for Transportation Materials and Methods of Sampling and Testing*, American Association of State Highway and Transportation Officials (AASHTO), Washington, D.C.

[2] AASHTO R 35, 2017. "Standard Practice for Superpave Volumetric Design for Asphalt Mixtures." *Standard Specifications for Transportation Materials and Methods of Sampling and Testing*, American Association of State Highway and Transportation Officials (AASHTO), Washington, D.C.

[3] AASHTO T 166, 2016. "Standard Method of Test for Bulk Specific Gravity (G_{mb}) of Compacted Hot Mix Asphalt (HMA) Using Saturated Surface-Dry Specimens." *Standard Specifications for Transportation Materials and Methods of Sampling and Testing*, American Association of State Highway and Transportation Officials (AASHTO), Washington, D.C.

[4] AASHTO T 209, 2020. "Standard Method of Test for Theoretical Maximum Specific Gravity (Gmm) and Density of Hot-Mix Asphalt (HMA)." *Standard Specifications for Transportation Materials and Methods of Sampling and Testing*, American Association of State Highway and Transportation Officials (AASHTO), Washington, D.C.

[5] AASHTO T 283, 2014. "Standard Method of Test for Resistance of Compacted Asphalt Mixtures to Moisture-Induced Damage." *Standard Specifications for Transportation Materials and Methods of Sampling and Testing*, American Association of State Highway and Transportation Officials (AASHTO), Washington, D.C.

[6] AASHTO T 316, 2019. "Standard Method of Test for Viscosity Determination of Asphalt Binder Using Rotational Viscometer." *Standard Specifications for Transportation Materials and Methods of Sampling and Testing*, American Association of State Highway and Transportation Officials (AASHTO), Washington, D.C.

[7] AASHTO T 324, 2019. "Standard Method of Test for Hamburg Wheel-Track Testing of Compacted Hot Mix Asphalt (HMA)." *Standard Specifications for Transportation Materials and Methods of Sampling and Testing*, American Association of State Highway and Transportation Officials (AASHTO), Washington, D.C.

[8] AASHTO T 361, 2016. "Standard Method of Test for Determining Asphalt Binder Bond Strength by Means of the Binder Bond Strength (BBS) Test." *Standard Specifications for Transportation Materials and Methods of Sampling and Testing*, American Association of State Highway and Transportation Officials (AASHTO), Washington, D.C.

[9] Airey, G.D. and Mohammed, M.H., 2008. "Rheological properties of polyacrylates used as synthetic road binders." *Rheologica Acta*, *47*(7), pp.751-763.

[10] Al-Qadi, I.L., Ozer, H., Lambros, J., El Khatib, A., Singhvi, P., Khan, T., Rivera-Perez, J. and Doll, B., 2015. "Testing protocols to ensure performance of high asphalt binder replacement mixes using RAP and RAS." Illinois Center for Transportation/Illinois Department of Transportation.

[11] Aman Mohammadi, M., Hosseini, S.M. and Yousefi, M., 2020. "Application of electrospinning technique in development of intelligent food packaging: A short review of recent trends." *Food Science & Nutrition*.

[12] Ameli, A., Khabbaz, E.H., Babagoli, R., Norouzi, N. and Valipourian, K., 2020. "Evaluation of the effect of carbon nano tube on water damage resistance of Stone matrix asphalt mixtures

containing polyphosphoric acid and styrene butadiene rubber." *Construction and Building Materials*, *261*, p.119946.

[13] Amirkhanian, A.N., Xiao, F. and Amirkhanian, S.N., 2011. "Characterization of unaged asphalt binder modified with carbon nano particles." *International Journal of Pavement Research and Technology*, *4*(5), p.281.

[14] ASTM D256, 2018. "Standard Test Methods for Determining the Izod Pendulum Impact Resistance of Plastics." *2018 Annual Book of ASTM Standards*, ASTM International, West Conshohocken, PA.

[15] ASTM D8044, 2016. "Standard Test Method for Evaluation of Asphalt Mixture Cracking Resistance using the Semi-Circular Bend Test (SCB) at Intermediate Temperatures." *2016 Annual Book of ASTM Standards*, ASTM International, West Conshohocken, PA.

[16] Birgisson, B., Roque, R., Tia, M. and Masad, E., 2005. "Development and evaluation of test methods to evaluate water damage and effectiveness of antistripping agents." *Chapters*, *2*(3), p.6.

[17] Biswas, M.C., Bush, B. and Ford, E., 2020. "Glucaric Acid Additives for the Antiplasticization of Fibers Wet Spun from Cellulose Acetate/Acetic Acid/Water." *Carbohydrate Polymers*, p. 116510.

[18] Casper, C. L., Stephens, J. S., Tassi, N. G., Chase, D. B., & Rabolt, J. F. (2004). "Controlling surface morphology of electrospun polystyrene fibers: effect of humidity and molecular weight in the electrospinning process." *Macromolecules*, 37(2), 573-578. DOI: 10.1021/ma0351975

[19] Daly, W.H., 2017. *Relationship Between Chemical Makeup of Binders and Engineering Performance* (No. Project 20-015 (Topic 47-13)).

[20] Eda, G., Liu, J. and Shivkumar, S., 2007. "Solvent effects on jet evolution during electrospinning of semi-dilute polystyrene solutions." *European Polymer Journal*, *43*(4), pp. 1154-1167.

[21] Fini, E.H., Hosseinnezhad, S., Oldham, D., Mclaughlin, Z., Alavi, Z. and Harvey, J., 2019. "Bio-modification of rubberised asphalt binder to enhance its performance." *International Journal of Pavement Engineering*, *20*(10), pp. 1216-1225.

[22] Fischer, S., Thümmler, K., Volkert, B., Hettrich, K., Schmidt, I. and Fischer, K., 2008, January. "Properties and applications of cellulose acetate." In *Macromolecular Symposia* (Vol. 262, No. 1, pp. 89-96). Weinheim: WILEY-VCH Verlag.

[23] Ghabchi, R., 2022. "Effect of Lignin Type as an Additive on Rheology and Adhesion Properties of Asphalt Binder." *Solids*, *3*(4), pp. 603-619.

[24] Ghabchi, R., Arshadi, A., Zaman, M. and March, F., 2021a. "Technical challenges of utilizing ground tire rubber in asphalt pavements in the United States." *Materials*, *14*(16), p. 4482.

[25] Ghabchi, R. and Castro, M.P.P., 2021a. "Evaluation of a biofuel residue-derived recycling agent with a low carbon footprint." *Transportation Engineering*, *5*, p.100085.

[26] Ghabchi, R. and Castro, M.P.P., 2021b. "Effect of laboratory-produced cellulose nanofiber as an additive on performance of asphalt binders and mixes." *Construction and Building Materials*, *286*, p. 122922.

[27] Ghabchi, R. and Castro, M.P., 2022. "Characterisation of a hybrid plant-based asphalt binder replacement with high reactive phenolic monomer content." *International Journal of Pavement Engineering*, *23*(13), pp. 4675-4696.

[28] Ghabchi, R., Rani, S., Zaman, M. and Ali, S.A., 2021b. "Effect of WMA additive on properties of PPA-modified asphalt binders containing anti-stripping agent." *International Journal of Pavement Engineering*, *22*(4), pp. 418-431.

[29] Ghabchi, R., Singh, D. and Zaman, M., 2014. "Evaluation of moisture susceptibility of asphalt mixes containing RAP and different types of aggregates and asphalt binders using the surface free energy method." *Construction and Building Materials*, *73*, pp. 479-489.

[30] Ghabchi, R., Singh, D., Zaman, M. and Hossain, Z., 2016. "Micro-structural analysis of moisture-induced damage potential of asphalt mixes containing RAP." *Journal of Testing and Evaluation*, *44*(1), pp. 194-205.

[31] Ghanoon, S.A., Tanzadeh, J. and Mirsepahi, M., 2020. "Laboratory evaluation of the composition of nano-clay, nano-lime and SBS modifiers on rutting resistance of asphalt binder." *Construction and Building Materials*, *238*, p. 117592.

[32] Hamedi, G.H., Ghahremani, H. and Saedi, D., 2020. "Investigation the effect of short term aging on thermodynamic parameters and thermal cracking of asphalt mixtures modified with nanomaterials." *Road Materials and Pavement Design*, pp. 1-28.

[33] Han, S.O., Youk, J.H., Min, K.D., Kang, Y.O. and Park, W.H., 2008. "Electrospinning of cellulose acetate nanofibers using a mixed solvent of acetic acid/water: Effects of solvent composition on the fiber diameter." *Materials Letters*, *62*(4-5), pp. 759-762.

[34] Hansen, K. R., and Copeland, A. (2017). "Asphalt pavement industry survey on recycled materials and warm-mix asphalt usage." Information Series 138, Report Submitted to: NAPA, Lanham, MD.

[35] Hanz, A., 2007. *Test Method to Determine Aggregate/Asphalt Adhesion Properties and Potential Moisture Damage*. University of Wisconsin-Madison, Madison, WI.

[36] Hossain, Z., Alam, M.S. and Baumgardner, G., 2020. "Evaluation of rheological performance and moisture susceptibility of polyphosphoric acid modified asphalt binders." *Road Materials and Pavement Design*, *21*(1), pp. 237-252.

[37] Hossain, Z., Zaman, M., Saha, M.C. and Hawa, T., 2014. "Evaluation of viscosity and rutting properties of nanoclay-modified asphalt binders." In *Geo-Congress 2014: Geo-characterization and Modeling for Sustainability* (pp. 3695-3702).

[38] Huang, Z. M., Zhang, Y. Z., Kotaki, M., & Ramakrishna, S. (2003). "A review on polymer nanofibers by electrospinning and their applications in nanocomposites." *Composites Science and Technology*, 63(15), 2223-2253. DOI: 10.1016/S0266-3538(03)00178-7

[39] Júnior, J.L.O.L., Babadopulos, L.F.D.A.L. and Soares, J.B., 2020. "Influence of Aggregate–Binder Adhesion on Fatigue Life of Asphalt Mixtures." *Journal of Testing and Evaluation*, *48*(1), pp. 150-160.

[40] Karnati, S.R., Oldham, D., Fini, E.H. and Zhang, L., 2020. "Application of surface-modified silica nanoparticles with dual silane coupling agents in bitumen for performance enhancement." *Construction and Building Materials*, *244*, p. 118324.

[41] Khattak, M.J., Khattab, A. and Rizvi, H.R., 2011. "Mechanistic characteristics of asphalt binder and asphalt matrix modified with nano-fibers." In *Geo-Frontiers 2011: Advances in Geotechnical Engineering* (pp. 4812-4822).

[42] Khattak, M.J., Khattab, A., Rizvi, H.R. and Zhang, P., 2012. "The impact of carbon nano-fiber modification on asphalt binder rheology." *Construction and Building Materials*, *30*, pp. 257-264.

[43] Kim, M., Mohammad, L.N. and Elseifi, M.A., 2012. "Characterization of fracture properties of asphalt mixtures as measured by semicircular bend test and indirect tension test." *Transportation research record*, *2296*(1), pp. 115-124.

[44] Kocak, S. and Kutay, M.E., 2020. "Fatigue performance assessment of recycled tire rubber modified asphalt mixtures using viscoelastic continuum damage analysis and AASHTOWare pavement ME design." *Construction and Building Materials*, *248*, p. 118658.

[45] Li, C., Han, X., Gong, J., Su, W., Xi, Z., Zhang, J., Wang, Q. and Xie, H., 2020. "Impact of waste cooking oil on the viscosity, microstructure and mechanical performance of warm-mix epoxy asphalt binder." *Construction and Building Materials*, *251*, p. 118994.

[46] Li, D., & Xia, Y. (2004). "Direct fabrication of composite and ceramic hollow nanofibers by electrospinning." *Nano Letters*, 4(5), 933-938. DOI: 10.1021/nl049590f

[47] Li, R., Xiao, F., Amirkhanian, S., You, Z. and Huang, J., 2017. "Developments of nano materials and technologies on asphalt materials–A review." *Construction and Building Materials*, *143*, pp. 633-648.

[48] Liu, H. and Hsieh, Y.L., 2002. "Ultrafine fibrous cellulose membranes from electrospinning of cellulose acetate." *Journal of Polymer Science Part B: Polymer Physics*, *40*(18), pp. 2119-2129.

[49] Liu, X., Yang, Y., Yu, D.G., Zhu, M.J., Zhao, M. and Williams, G.R., 2019. "Tunable zero-order drug delivery systems created by modified triaxial electrospinning." *Chemical Engineering Journal*, *356*, pp. 886-894.

[50] Lu, Q. and Harvey, J.T., 2006. "Evaluation of Hamburg wheel-tracking device test with laboratory and field performance data." *Transportation Research Record*, *1970*(1), pp. 25-44.

[51] Mehta, P., Haj-Ahmad, R., Rasekh, M., Arshad, M.S., Smith, A., van der Merwe, S.M., Li, X., Chang, M.W. and Ahmad, Z., 2017. "Pharmaceutical and biomaterial engineering via electrohydrodynamic atomization technologies." *Drug Discovery Today*, *22*(1), pp. 157-165.

[52] Mo, L.T., Huurman, M., Woldekidan, M.F., Wu, S.P. and Molenaar, A.A., 2010. "Investigation into material optimization and development for improved ravelling resistant porous asphalt concrete." *Materials & Design*, *31*(7), pp. 3194-3206.

[53] Nejad, F.M., Aflaki, E. and Mohammadi, M.A., 2010. "Fatigue behavior of SMA and HMA mixtures." *Construction and Building Materials*, *24*(7), pp. 1158-1165.

[54] Mohammad, L.N., Kim, M. and Elseifi, M., 2012. "Characterization of asphalt mixture's fracture resistance using the semi-circular bending (SCB) test." In 7th RILEM International Conference on Cracking in Pavements (pp. 1-10). Springer, Dordrecht.

[55] Mohammad, L.N., Wu, Z. and Aglan, M.A., 2004, May. "Characterization of fracture and fatigue resistance on recycled polymer-modified asphalt pavements." In Proceedings, 5th International Conference (pp. 375-382).

[56] Moraes, R., Velasquez, R. and Bahia, H.U., 2011. "Measuring the effect of moisture on asphalt–aggregate bond with the bitumen bond strength test." *Transportation Research Record*, *2209*(1), pp. 70-81.

[57] Oishi, Y., Nakaya, M., Matsui, E. and Hotta, A., 2015. "Structural and mechanical properties of cellulose composites made of isolated cellulose nanofibers and poly (vinyl alcohol)." *Composites Part A: Applied Science and Manufacturing*, *73*, pp. 72-79.

[58] Ozer, H., Al-Qadi, I.L., Singhvi, P., Bausano, J., Carvalho, R., Li, X. and Gibson, N., 2018. "Prediction of pavement fatigue cracking at an accelerated testing section using asphalt mixture performance tests." *International Journal of Pavement Engineering*, *19*(3), pp. 264-278.

[59] Sarkar, M.T.A., Rahman, M.N., Elseifi, M.A., Mayeux, C. and Cooper III, S.B., 2020. "Rheological and Molecular Characterizations of Tire Rubber Modified Asphalt Emulsion." *Transportation Research Record*, *2674*(3), pp. 12-26.

[60] Shafabakhsh, G.A., Sadeghnejad, M., Ahoor, B. and Taheri, E., 2020. "Laboratory experiment on the effect of nano SiO2 and TiO2 on short and long-term aging behavior of bitumen." *Construction and Building Materials*, *237*, p. 117640.

[61] Sheng, X., Xu, T. and Wang, M., 2020. "Preparation, shape memory performance and microstructures of emulsified asphalt modified by multi-walled carbon nanotubes." *Construction and Building Materials*, *230*, p. 116954.

[62] Smit, E., Bűttner, U. and Sanderson, R.D., 2005. "Continuous yarns from electrospun fibers." *Polymer*, *46*(8), pp. 2419-2423.

[63] Son, W.K., Youk, J.H., Lee, T.S. and Park, W.H., 2004. "Electrospinning of ultrafine cellulose acetate fibers: studies of a new solvent system and deacetylation of ultrafine cellulose acetate fibers." *Journal of Polymer Science Part B: Polymer Physics*, *42*(1), pp. 5-11.

[64] Su, M., Si, C., Zhang, Z., and Zhang, H., 2020. "Molecular dynamics study on influence of Nano-ZnO/SBS on physical properties and molecular structure of asphalt binder." *Fuel*, *263*, p. 116777.

[65] Subbiah, T., Bhat, G.S., Tock, R.W., Parameswaran, S. and Ramkumar, S.S., 2005. "Electrospinning of nanofibers." *Journal of Applied Polymer Science*, *96*(2), pp. 557-569.

[66] Sun, Z., Yi, J., Huang, Y., Feng, D. and Guo, C., 2016. "Properties of asphalt binder modified by bio-oil derived from waste cooking oil." *Construction and Building Materials*, *102*, pp. 496-504.

[67] Teo, W. E., & Ramakrishna, S. (2006). "A review on electrospinning design and nanofibre assemblies." *Nanotechnology*, 17(14), R89. DOI: 10.1088/0957-4484/17/14/R01

[68] Thompson, C. J., Chase, G. G., Yarin, A. L., & Reneker, D. H. (2007). "Effects of parameters on nanofiber diameter determined from electrospinning model." *Polymer*, 48(23), 6913-6922. DOI: 10.1016/j.polymer.2007.09.017

[69] Toraldo, E. and Mariani, E., 2014. "Effects of polymer additives on bituminous mixtures." *Construction and Building Materials*, *65*, pp. 38-42.

[70] Tungprapa, S., Puangparn, T., Weerasombut, M., Jangchud, I., Fakum, P., Semongkhol, S., Meechaisue, C. and Supaphol, P., 2007. "Electrospun cellulose acetate fibers: effect of solvent system on morphology and fiber diameter." *Cellulose*, *14*(6), pp. 563-575.

[71] Wang, P., Dong, Z.J., Tan, Y.Q. and Liu, Z.Y., 2017. "Effect of multi-walled carbon nanotubes on the performance of styrene–butadiene–styrene copolymer modified asphalt." *Materials and Structures*, *50*(1), p. 17.

[72] Wen, H., Bhusal, S. and Wen, B., 2013. "Laboratory evaluation of waste cooking oil-based bioasphalt as an alternative binder for hot mix asphalt." *Journal of Materials in Civil Engineering*, *25*(10), pp. 1432-1437.

[73] Williams, B.A., Willis, J.R., and Shacat, J., 2024. "Asphalt Pavement Industry Survey on Recycled Materials and Warm-Mix Asphalt Usage: 2022" (Information Series 138) (13th ed.) National Asphalt Pavement Association (NAPA), 6406 Ivy Lane, Suite 350, Greenbelt, MD 20770-1441.

[74] Wu, S., Ye, Q., Li, N. and Yue, H., 2007. "Effects of fibers on the dynamic properties of asphalt mixtures." *Journal of Wuhan University of Technology-Mater. Sci. Ed.*, *22*(4), pp. 733-736.

[75] Xiao, F., Amirkhanian, S., Wang, H. and Hao, P., 2014. “Rheological property investigations for polymer and polyphosphoric acid modified asphalt binders at high temperatures.” *Construction and Building Materials*, *64*, pp. 316-323.

[76] Xin, X., Liang, M., Yao, Z., Su, L., Zhang, J., Li, P., Sun, C. and Jiang, H., 2020. “Self-sensing behavior and mechanical properties of carbon nanotubes/epoxy resin composite for asphalt pavement strain monitoring.” *Construction and Building Materials*, *257*, p. 119404.

[77] Yang, Q., Li, X., Zhang, L., Qian, Y., Qi, Y., Kouhestani, H.S., Shi, X., Gui, X., Wang, D. and Zhong, J., 2020. “Performance evaluation of bitumen with a homogeneous dispersion of carbon nanotubes.” *Carbon*, *158*, pp. 465-471.

[78] Yildirim, Y., 2007. “Polymer modified asphalt binders.” *Construction and Building Materials*, *21*(1), pp. 66-72.

[79] Yu, H., Zhu, Z., Leng, Z., Wu, C., Zhang, Z., Wang, D. and Oeser, M., 2020. “Effect of mixing sequence on asphalt mixtures containing waste tire rubber and warm mix surfactants.” *Journal of Cleaner Production*, *246*, p. 119008.

[80] Ziari, H., Aliha, M.R.M., Moniri, A. and Saghafi, Y., 2020. “Crack resistance of hot mix asphalt containing different percentages of reclaimed asphalt pavement and glass fiber.” *Construction and Building Materials*, *230*, p. 117015.

[81] Ziari, H., Farahani, H., Goli, A. and Sadeghpour Galooyak, S., 2014. “The investigation of the impact of carbon nano tube on bitumen and HMA performance.” *Petroleum Science and Technology*, *32*(17), pp. 2102-2108.